ASTRONOMY & ASTROPHYSICS
SUPPLEMENT SERIES

Astron. Astrophys. Suppl. Ser. **52,** 63-103 (1983)

The gas distribution in the central region of the Galaxy. IV. A survey of neutral hydrogen in the region $349° \leq l \leq 13°$, $-10° \leq b \leq 10°$, $\mid v \mid \leq 350$ km.s^{-1}

W. B. Burton and H. S. Liszt (*)

Sterrewacht, Huygens Laboratorium, Wassenaarseweg 78, Postbus 9513, 2300 RA Leiden, the Netherlands

Received July 19, accepted November 2, 1982

Summary. — Presented here are 21-cm observations of neutral hydrogen emission from the core of our galaxy made over a period of several years with the 140-foot telescope of the National Radio Astronomy Observatory. The material covers the region $349° \leq l \leq 13°$, $-10° \leq b \leq 10°$, at intervals of one-half degree in both l and b. Each reduced spectrum covers the velocity range $\mid v \mid < 350$ km.s^{-1} at a kinematic resolution of 5.5 km.s^{-1} to an rms sensitivity limit ≥ 0.02 K. The data are displayed in three sets of representative maps drawn in latitude-longitude, latitude-velocity, and longitude-velocity coordinates. Anomalous features representing material in the galactic core are labelled in the appropriate figures. We give here some summarizing taxonomic remarks concerning these anomalies ; our own interpretation of this survey is the subject of the other papers in this series.

Key words : galaxies : nuclei — galaxies : Milky Way — galaxies : structure — interstellar : matter — radio sources : 21-cm radiation.

1. **Introduction.** — Evidence for anomalous behaviour of HI gas in the inner parts of our galaxy is well-documented (see Oort's 1977 review). The anomalous behaviour includes deviations from the kinematics consistent with axisymmetric motions as well as deviations from structural symmetry. The length scales involved range from some kpc in the case of the 3-kpc arm to the unresolved subparsec domain in the nucleus itself. The variety of observational characteristics is large and no doubt a variety of dynamical interpretations will have to be found to explain all of them.

The region interior to the 3-kpc arm but away from the nucleus itself has been extensively studied using the 21-cm line of HI. The pioneering work of Rougoor and Oort (1960) and Rougoor (1964) established that this region is pervaded by emission features moving at forbidden velocities and in some cases located at large z-distances. The observational work of identifying such features was extended in a number of HI surveys, particularly those of van der Kruit (1970) and Cohen (1975).

Our motivation for undertaking this observing program was essentially twofold. First, we wished to extend the velocity coverage beyond what was available. The spectral region at $\mid v \mid \gtrsim 250$ km.s^{-1} had not been surveyed to a sensitivity better than a few 0.1 K except in a few restricted regions. If the anomalous features have their origin in ejection from the nucleus, then higher velocities would be expected ; Oort (1977) emphasized that if the only restraint on a gas clouds's motion is the galactic gravitational field, then an initial velocity of some 700 km.s^{-1} is necessary for a cloud ejected from the nucleus to reach the heights observed of $z \approx 500$ pc. Second, we wished to extend the angular coverage, especially in latitude. It had become clear that the anomalous material extends to at least $\mid b \mid \sim 6°$, and to at least $\mid l \mid \sim 8°$. Furthermore, a number of earlier investigations had found structures inclined to the galactic plane. This result indicated the need for additional data away from the well-observed plane $b = 0°$. Thus Kerr (1967) had shown that HI emission at the extreme permitted velocities originates preferentially from the opposed quadrants $l > 0°$, $b < 0°$ and $l < 0°$, $b > 0°$. Shane (see Oort, 1968) had noted this same tendency for the more moderate velocities. Kerr and Sinclair (1966) showed that a ridge line in the 20-cm continuum flux is inclined in the same sense. It was noted by van der Kruit (1970) and discussed with emphasis by Cohen (1975) and by Cohen and Davis (1976) that the apparently isolated HI features at forbidden velocities also occur preferentially in these two opposed quadrants. This was taken as evidence of a favored collimation axis for nuclear activity. Subsequent work by Cohen (1979), by Sinha (1979a, b, c), and by us has stressed the tilted nature of the core HI emission.

Our own work on this subject has been reported in earlier papers in this series. In paper I (Burton and Liszt,

(*) Permanent address : National Radio Astronomy Observatory, which is operated by Associated Universities, Inc., under contract with the National Science Foundation.

1978), which was based on data from an exploratory version of this survey (Burton *et al.*, 1977), we showed that the tilted distribution encompassed essentially all of the HI gas, whether at forbidden or permitted velocities, within 2 kpc of the nucleus. In paper II (Liszt and Burton, 1978), we argued that the molecular gas, traced by observations of the 2.6-mm line of CO, also partakes in the systematic deviations from the equator. In paper III (Liszt and Burton, 1980), we showed that a tilted-bar model could account for the appearance of a diverse assortment of individual condensations in the observed position-velocity maps ; although this *ad hoc* model lacked dynamical foundation, we hoped that the paper might focus attention on the important need to decide between explanations of the core phenomena based on models requiring ejection from the galactic nucleus and those based on motions governed by the gravitational field.

The value of the data contributed here lies mainly in the broad velocity coverage at moderately high velocity resolution, in the sensitivity, and in the extent (but not in the density or resolution) of the positional coverage. Other HI surveys are superior to this one for some purposes. Table I summarizes the observational parameters and chief uses of surveys of the 21-cm line which preceed this one. Although HI has been the tracer which has revealed the most information on the gas in the core region (200 pc $\lesssim R \lesssim$ 3 kpc), information from surveys of other tracers, which we summarize in the other tables, must also be incorporated into any successful synthesis. For completeness, and because it is not yet clear that phenomena occurring in the nucleus itself are not associated with (or even responsible for) the characteristics in the core region, we also compile in the tables information on some observational studies pertaining to the smaller-scale phenomena. The somewhat subjective criteria used in compiling the tables stressed morphological aspects of the core gas.

2. **Observations.** — The observations were made on the NRAO 140-foot (43-m) telescope during four sessions. These sessions occurred in March, 1976 ; in January, February, and March, 1977 ; in August 1978 ; and in October and November, 1978, and comprised a total of 45 days during which the observing system functioned well. During the four sessions the parameters of the observing system were similar, producing a homogeneous set of data. The telescope was equipped with a cooled parametric amplifier of 50 K system temperature and a 384-channel auto-correlation spectrometer set to a total bandpass of 5 MHz centered at the local standard of rest zero velocity. We operated in the frequency-switching mode. After dropping the extreme 20 channels (unreliable because of the non-square response of the bandpass), the instrumental baseline was accounted for by a polynomial of order three or less found by least-squares fitting to portions of the profile wings judged by separate inspection of each profile to contain negligible emission.

The observations covered the velocity range $-500 < v < 500$ km.s^{-1} ; velocities in this paper are expressed relative to the local standard of rest motion of 20 km.s^{-1} toward α, $\delta = 18^{h}$, $+30°$ (epoch 1900.0). Because the observations show no emission near the borders of this range, our displays are restricted to $|v| < 350$ km.s^{-1} and include all perceived emission. Coming from the spectrometer, the velocity resolution of the data was 2.75 km.s^{-1}. Features in the galactic core are characterized by broad widths but low intensities ; consequently we enhanced the sensitivity of the spectra by degrading the velocity resolution to 5.5 km.s^{-1} using a digital filter.

The sensitivity of the data generally corresponds to an antenna-temperature rms level of 0.02 K or better. In regions away from the continuum background concentrated near the galactic equator, integration times of 600 s sufficed to maintain this level. Strong continuum sources near the equator raised the total system temperature and therefore necessitated longer integration times to achieve the desired sensitivity ; at $l = 0°$, $b = 0°$ we integrated for 6160 s and at the neighboring positions we integrated for about 1200 s. Longer-than-average integration times gave an rms level of about 0.01 K for about one third of the observed grid positions. The enhanced-sensitivity positions lie in the region where the characteristic signature of the galactic core emission is pronounced, defined during the observing sessions as a swath of 7-degree width running from $l < 0°$, $b > 0°$ to $l > 0°$, $b < 0°$, at an angle in l of approximately 20° measured from $b = 0°$. The lowest-level contour plotted in the position-velocity maps is 0.10 K. Inspection of the lowest contour in the maps gives a qualitative impression of the peak-to-peak noise level and provides a good criterion for interpretation of low-level features ; such inspection also reveals the enhanced-sensitivity swath.

The intensity units in the plots refer to antenna temperature. Formal conversion of antenna temperatures to the physically more important brightness temperatures requires more knowledge than is available about the 140-foot telescope and about the gas distribution in the inner galaxy. Antenna temperatures suffice for many uses of the data, including the principal one of identification of kinematic patterns. The most practical approach to temperature scaling involves following the IAU Commission 40 recommendation (van Woerden, 1970) to calibrate HI survey material to standard fields. The reference field S9, at $l \equiv 356°$, $b \equiv 4°$, lies within the region surveyed. Williams (1973) has discussed the conversion to brightness temperature appropriate for the Hat Creek 85-foot telescope, incorporating properties of that antenna and of the source distribution. We accept his S9 profile as the definition of the standard. The field was measured at the 140-foot on 9 occasions scattered throughout the observing sessions when the field was at approximately the same zenith angle. This produced a high quality spectrum and a reassurance of the stability of the observing system. From the mean spectrum we calculated the mean peak T_A, 59 ± 2 K, and the integral over the range $1.05 \leq v \leq 14.75$ km.s^{-1}, 598 ± 37 K.km.s^{-1}, and compared this to the corresponding values in the T_b scale of Williams. The ratio of peak intensities in T_A (140-foot)/T_b (Williams) = 0.69 ± 0.05 ; the ratio of the indicated integrals is $\int T_A$ (140-foot) dv/$\int T_b$ (Williams) dv = 0.63 ± 0.03. Calibration profiles of several standard regions have also been published by Pöppel and Vieira (1973). The ratio of peak temperatures is T_A (140-foot)/T_b (P & V) = 59/80 = 0.74 ; the ratio of total-velocity integrals is $\int T_A$ (140-foot) dv/

$\int T_b$ (P & V) dv = 1089/1547 = 0.70. We note that the intensity scale of Pöppel and Vieira for the S9 field differs from that of Williams, which we are accepting here. In both cases, however, our peak temperature measurement is higher than would be indicated by the integral comparisons. The higher resolution of the 140-foot telescope compared to that of the Hat Creek or Argentine telescope would tend toward a relative overestimate of the peak temperature comparison factor ; the broader channel spacing would have the opposite tendency. Therefore we give more weight to the comparison of integrals, which is, in any case, a comparison based on more data. The S9 field lies in a region of rapidly varying intensity. The $l = -4.^\circ0$ contour map in figure 3q shows this and also shows that the main peak of the S9 profile is rather narrow. An ideal standard field (and, indeed, the IAU recommendation names S9 as a secondary standard) would have a flat top (to ease determination of the peak T_A) and steep sides (to ease determination of correct velocity adjustment). We also compared the total-velocity integrals of profiles from the current survey with the corresponding integrals from profiles at integer longitudes in the galactic equator in the Parkes (Kerr *et al.*, 1981) and in the Bonn (Westerhout, 1976) surveys. The Parkes intensities are presented in nominal brightness-temperature units ; the Bonn intensities were converted using the factor 1.39. The ratio $\int T_A$ (140-foot) $dv / \int T_b$ (Parkes or Bonn) dv = 0.67 ± 0.02.

In view of the above we suggest for the present data the conversion $T_A = 0.66\ T_b$. In brightness temperature units, the lowest-level contour in the position-velocity maps corresponds to T_b = 0.15 K. The lowest-level contours plotted in the position-position maps vary for convenience according to the velocity range. Calculated for a representative 3 σ brightness temperature level of 0.05 K per 5.5 km.s^{-1} channel width under the plausible assumption that the optical depths of the core hydrogen are low, the minimum detectable column density value is 5.0×10^{17} cm^{-2}.

The principal value of the data in this contribution lies in the extent of the observed grid. In order to include all of the emission whose kinematic signature indicates that it is associated with the galactic core, an extent to at least $|b| = 8^\circ$ is necessary. An even greater extent is necessary in l : the 3-kpc arm extends to $l < 348^\circ$, the so-called connecting arm extends beyond $l \approx 15^\circ$, and the tilted distribution in which we are particularly interested extends to $|l| \sim 8^\circ$ at least. These observations were made on a grid which extends from $b = 10^\circ$ to -10°, and from $= -11^\circ$ to 13°. Such an extensive grid precludes a dense one : the grid interval here is one-half degree in both l and b. The data are thus undersampled by the 21′ beam of the 140-foot telescope. Essentially all of the emission patterns associated with the galactic core, however, extend over angles of a degree or more on the sky. The maps presented here bear out this characteristic ; it is also supported by the higher-resolution material available in some subregions of the core (see Table I). Therefore, we believe that the effective resolution set mainly by the grid interval is not detrimental in the respect of resolution of angular extent on the sky. The resolution is limiting, however, for those emission patterns which show a large velocity gradient effective on a small angular scale. Such patterns are not unusual, occurring near the nucleus as well as in the outer regions of the core. The most realistic way to study these features with resolution improved by more than a factor of a few will probably involve observations of spectral lines of molecules, especially CO.

3. **Data.** — Representative cuts through the data cube are displayed in figures 1 and 2 as l, b maps over the indicated velocity ranges, in figure 3 as b, v maps at constant l, and in figure 4 as l, v maps at constant b. In the position coordinates of these maps, the observed spectra are separated by 0.°5 ; in the velocity coordinates, the separation is 5.5 km.s^{-1}. In figures 1 and 2, the contours are labelled in units of K.km.s^{-1} ; a contour level of 100 K.km.s^{-1} surrounding one square degree corresponds to emission from $6.3 \times 10^4\ M_\odot$ of HI if the gas lies at a distance of 10 kpc and is optically transparent. In figures 3 and 4, the contours are drawn at the levels T_A = 0.1, 0.23, 0.4, 0.9, 1.7, 3, 6, 10, 15, 25, 35, ... K. Hatched contours enclose regions of relatively low antenna temperatures.

The known anomalous features presumably associated with the central region are labelled in the appropriate figures. Many of these features have been discussed by several authors, and some of the features are referred to in the literature by more than one name. We have tried to label each feature in accordance with the earliest publication which treats it as a separate entity. The references pertain to the relevant observational, as opposed to interpretive, papers. A number of additional features are pointed out in the figures but not labelled. These represent features which have not yet been discussed separately in the literature or which appear for the first time in these observations. Some of these features appear to be low-level extensions of previously discussed features.

Figure 1 comprises two spatial maps of the antenna temperatures integrated over the indicated, wide velocity ranges. These maps summarize the well-known tendency of the integrated emission from the central region to depart coherently from the $b = 0^\circ$ plane on both sides of $l = 0^\circ$, irrespective of the forbidden or permitted nature of the velocities. The range of integration is broken into smaller intervals in the spatial maps comprising figure 2. Unambiguously « forbidden » material is only isolated at $l < 0^\circ$ in the positive-velocity maps and at $l > 0^\circ$ in the negative-velocity ones. Some of the emission is no doubt contributed by gas lying outside of the core of the galaxy ; emission at moderate velocities at $|l| \gtrsim 8^\circ$ and confined near $b = 0^\circ$ is certainly dominated by such gas. Nevertheless the anomalous behaviour of many features at the formally « permitted » velocities has been well established by their characteristics in position, velocity space. Irrespective of the forbidden or permitted nature of the velocities, most of the anomalous emission shares a coherent skewness. Pointers in figure 2 show the locations of the principal anomalous features, but not in much detail because the ranges of integration chosen do not necessarily isolate the individual features in an optimal way.

The individual features are most easily studied using position, velocity maps. Figure 3 gives b, v maps at one-

degree intervals in l over $-11° < l < 12°$. Figure 4 gives the l, v maps at one-degree invals in b over $-6° < b < 6°$. Experience has suggested to us that the detailed kinematics of the core gas are revealed somewhat more clearly in longitude, velocity maps formed at constant latitudes than in latitude, velocity maps ; the signature of the inner-galaxy disk varies more slowly with position and velocity in l, v diagrams and there is generally less contamination (except at $|b| \lesssim 1°$) in these diagrams from transgalactic gas.

4. **Summary comments.** — Our own interpretation of the material in this survey is the subject of other papers in this series. In view of the extensive discussions of the individual anomalous features given in the detection papers referenced in the figure legends, in the interpretative papers referenced in table I, as well as in papers I and III of this series, only a few generalizations need be noted here.

The taxonomy of the anomalous-velocity HI features located between a few hundred pc and a few kpc of the galactic center share the following characteristics :

1. *The anomalous-velocity features, and the core HI in general, lie in a tilted distribution.* A wide variety of work supports this conclusion for the anomalous-velocity features in the region 200 pc $\lesssim R \lesssim$ 3 kpc. We believe it may be generalized to include the conventional-velocity gas. We note in particular the skewed symmetry of the « connecting arm » gas (see Figs. 3g and 3h) and the « nuclear disk » gas (see Figs. 3r and 3s).

2. *The anomalous-velocity features, and the core HI in general, are confined within a definite kinematic envelope.* In this sense the anomalous kinematics are well-behaved. The location of the envelope is given roughly by the outermost contour in figure 5a of paper III, an l, v diagram of observations made along the approximate principal plane of the tilted distribution (Shane's feature, e.g. figure 2g, is an exception to this confinement). We note that this survey detected no previously unknown emission feature at $|v| > 150$ km.s^{-1}, even though velocities to $|v| = 500$ km.s^{-1} were searched.

3. *The anomalous-velocity features show substantial continuity in position and in velocity.* It seems to us easier to argue that the anomalous and conventional material together more or less fill the envelope region than that the various anomalous features are isolated. An example of such continuity is given by the apparent merging of features XII, X, E, SWP, and SWa (see e.g. Figs. 4j and 4k) ; continuity across the confused region near $v = 0$ km.s^{-1} is suggested by the behaviour of features J5 and XII (see e.g. Fig. 4k) and features SWb and its negative-velocity counterpart (see e.g. Fig. 4d).

4. *The major anomalous-velocity features occur in positive- and negative-velocity pairs.* This tendency is most easily recognized in the constant-latitude maps of figure 4, for example those at $b = \pm 3.^{\circ}0$. The velocity pairing occurs within the same l, b quadrant. This is not the situation which might be expected for oppositely-directed streams from a single nuclear ejection, for which the resulting pairing would be to opposite l, b quadrants.

5. *The anomalous-velocity features all show exceptionally large velocity dispersions.* This has been recognized by all investigators. The large σ_v, > 50 km.s^{-1} typically, hold for the HI emission as well as for the absorption spectra, and therefore refer to a wide range of length scales on the sky. The presumably very cold molecular gas (cf. Paper II) shows comparable dispersions. The profile shapes are very non-gaussian ; the wings of the spectral features often terminate sharply. We believe that the dispersion characteristics are more plausibly due to long paths through a more-or-less filled distribution with large perceived velocity gradients than they are to intrinsic properties of isolated gas clumps.

The characteristics summarized here constitute the most important aspects of the signature of the core HI which syntheses should address. Different constraints, of course, apply to gas (mostly studied in molecular lines) interior to $R \sim 200$ pc and to gas (most obviously the 3-kpc arm) exterior to $R \sim 3$ kpc.

Acknowledgements. — W. B. Burton acknowledges support for some of this work at the University of Minnesota from the U.S. National Science Foundation through grant AST-7921812. We gratefully acknowledge support from the North Atlantic Treaty Organization through Research Grant No. 008.82, which made possible H. S. Liszt's work at the Leiden Sterrewacht.

References

AITKEN, D. K., JONES, B. and PENMAN, J. M. : 1974, *Mon. Not. R. Astron. Soc.* **169**, 35.
ALTENHOFF, W. J., DOWNES, D., GOAD, L., MAXWELL, A. and RINEHART, R. : 1970, *Astron. Astrophys. Suppl. Ser.* **1**, 319.
ALTENHOFF, W. J., DOWNES, D., PAULS, T. and SCHRAML, J. : 1979, *Astron. Astrophys. Suppl. Ser.* **35**, 23.
BALICK, B. and BROWN, R. L. : 1974, *Astrophys. J.* **194**, 265.
BALICK, B. and SANDERS, R. H. : 1974, *Astrophys. J.* **191**, 325.
BANIA, T. M. : 1977, *Astrophys. J.* **216**, 381.
BANIA, T. M. : 1980, *Astrophys. J.* **242**, 95.
BAUD, B., HABING, H. J., MATTHEWS, H. E. and WINNBERG, A. : 1979, *Astron. Astrophys. Suppl. Ser.* **35**, 179.
BECKLIN, E. E. and NEUGEBAUER, G. : 1968, *Astrophys. J.* **151**, 145.
BECKLIN, E. E. and NEUGEBAUER, G. : 1975, *Astrophys. J.* **200**, L71.
BECKLIN, E. E., MATTHEWS, K., NEUGEBAUER, G. and WILLNER, S. P. : 1978, *Astrophys. J.* **219**, 121.
BIEGING, J. H. : 1976, *Astron. Astrophys.* **51**, 289.
BIEGING, J. H., DOWNES, D., WILSON, T. L., MARTIN, A. H. M. and GÜSTEN, R. : 1980, *Astron. Astrophys. Suppl. Ser.* **42**, 163.
BRAUNSFURTH, E. and ROHLFS, K. : 1981, *Astron. Astrophys. Suppl. Ser.* **44**, 437.
BROWN, R. L., JOHNSTON, K. J. and LO, K. Y. : 1981, *Astrophys. J.* **250**, 155.

BROWN, R. L., LO, K. Y. and JOHNSTON, K. J. : 1978, *Astron. J.* **83,** 1594.
BURTON, W. B. : 1970, *Astron. Astrophys. Suppl. Ser.* **2,** 261.
BURTON, W. B. : 1971, *Astron. Astrophys.* **10,** 76.
BURTON, W. B. and LISZT, H. S. : 1978, *Astrophys. J.* **225,** 815 (Paper I).
BURTON, W. B. and LISZT, H. S. : 1981, *Proc. I.A.U. Symp.* **94,** 227.
BURTON, W. B., GALLAGHER, J. S. and MCGRATH, M. A. : 1977, *Astron. Astrophys. Suppl. Ser.* **29,** 123.
COHEN, R. J. : 1975, *Mon. Not. R. Astron. Soc.* **171,** 659.
COHEN, R. J. : 1977, *Mon. Not. R. Astron. Soc.* **178,** 547.
COHEN, R. J. : 1979, *Proc. I. A. U. Symp.* **84,** 337.
COHEN, R. J. and DAVIES, R. D. : 1976, *Mon. Not. R. Astron. Soc.* **175,** 1.
COHEN, R. J. and DAVIES, R. D. : 1979, *Mon. Not. R. Astron. Soc.* **186,** 453.
COHEN, R. J. and FEW, R. W. : 1976, *Mon. Not. R. Astron. Soc.* **176,** 495.
COHEN, R. J. and FEW, R. W. : 1981, *Mon. Not. R. Astron. Soc.* **194,** 711.
CUGNON, P. : 1968, *Bull. Astron. Inst. Netherl.* **19,** 363.
DAVIES, R. D., WALSH, D. and BOOTH, R. S. : 1976, *Mon. Not. R. Astron. Soc.* **177,** 319.
D'ODORICO, S., SANCISI, R. and SIMONSON, S. C. : 1969, *Astron. Astrophys.* **1,** 131.
DOWNES, D., GOSS, W. M., SCHWARZ, U. J. and WOUTERLOOT, J. G. A. : 1978, *Astron. Astrophys. Suppl. Ser.* **35,** 1.
DOWNES, D. and MAXWELL, A. : 1966, *Astrophys. J.* **146,** 653.
EKERS, R. D., GOSS, W. M., SCHWARZ, U., DOWNES, D. and ROGSTAD, D. H. : 1975, *Astron. Astrophys.* **43,** 159.
EKERS, R. D. and SCHWARZ, U. : 1982, in preparation.
FUKUI, Y., KAIFU, N., MORIMOTO, M. and MIYAJI, T. : 1980, *Astrophys. J.* **241,** 147.
FUKUI, Y., IGUCHI, T., KAIFU, N., CHIKADA, Y., MORIMOTO, M., NAGANE, K., MIYAZAWA, K. and MIYAJI, T. : 1977, *Publ. Astron. Soc. Japan* **29,** 643.
GÜSTEN, R. and DOWNES, D. : 1980, *Astron. Astrophys.* **87,** 6.
HARRIS, A. W., LEMKE, D. and HOFMANN, W. : 1980, *Astrophys. Space Sci.* **72,** 111.
HARVEY, P. M., CAMPBELL, M. F. and HOFFMAN, W. F. : 1976, *Astrophys. J.* **205,** L69.
HAYAKAWA, S., MATSUMOTO, T., MURAKAMI, H., UYAMA, K., THOMAS, J. A. and YAMAGAMI, T. : 1981, *Astron. Astrophys.* **100,** 116.
HAYAKAWA, S., MATSUMOTO, T., MURAKAMI, H., UYAMA, K., YAMAGAMI, T. and THOMAS, J. A. : 1979, *Nature* **279,** 510.
HILDEBRAND, R. H., WHITCOMB, S. E., WINSTON, R., STIENING, R. F., HARPER, D. A. and MOSELEY, S. H. : 1978, *Astrophys. J.* **219,** L101.
HOFFMAN, W. F., FREDERICK, C. L. and EMERY, R. J. : 1971, *Astrophys. J.* **164,** L23.
HOFMANN, W., LEMKE, D. and FREY, A. : 1978, *Astron. Astrophys.* **70,** 427.
HULSBOSCH, A. N. M. : 1968, *Bull. Astron. Inst. Netherl.* **20,** 33.
INATANI, J. : 1980, *Publ. Astron. Soc. Japan,* preprint.
ITO, K., MATSUMOTO, T. and UYAMA, K. : 1977, *Nature* **265,** 517.
KELLERMANN, K. I., SHAFFER, D. B., CLARK, B. G. and GELDZAHLER, B. J. : 1977, *Astrophys. J.* **214,** L61.
KERR, F. J. : 1967, *Proc. I. A. U. Symp.* **31,** 219.
KERR, F. J. : 1969, *Aust. J. Phys., Astrophys. Suppl.* **9.**
KERR, F. J. and HINDMAN, J. V. : 1970, *Aust. J. Phys., Astrophys. Suppl.* **18,** 1.
KERR, F. J. and SINCLAIR, M. W. : 1966, *Nature* **212,** 166.
KERR, F. J. and VALLAK, R. : 1967, *Aust. J. Phys., Astrophys. Suppl.* **3,** 1.
KERR, F. J., BOWERS, P. F. and HENDERSON, A. P. : 1981, *Astron. Astrophys. Suppl. Ser.* **44,** 63.
LACY, J. H., BAAS, F., TOWNES, C. H. and GEBALLE, T. R. : 1979, *Astrophys. J.* **227,** L17.
LACY, J. H., TOWNES, C. H., GEBALLE, T. R. and HOLLENBACH, D. J. : 1980, *Astrophys. J.* **241,** 132.
LINDBLAD, P. O. : 1974, *Astron. Astrophys. Suppl. Ser.* **16,** 207.
LINKE, R. A., STARK, A. A. and FRERKING, M. A. : 1980, *Astrophys. J.* **235,** 840.
LINKE, R. A., STARK, A. A. and FRERKING, M. A. : 1981, *Astrophys. J.* **243,** 147.
LISZT, H. S. and BURTON, W. B. : 1978, *Astrophys. J.* **226,** 790 (Paper II).
LISZT, H. S. and BURTON, W. B. : 1980, *Astrophys. J.* **236,** 779 (Paper III).
LISZT, H. S. and BURTON, W. B. : 1982, in preparation.
LISZT, H. S., BURTON, W. B., SANDERS, R. H. and SCOVILLE, N. Z. : 1977, *Astrophys. J.* **213,** 38.
LISZT, H. S., SANDERS, R. H. and BURTON, W. B. : 1975, *Astrophys. J.* **198,** 537.
LISZT, H. S., VAN DER HULST, J. M., ONDRECHEN, M. and BURTON, W. B. : 1982, in preparation.
LITTLE, A. G. : 1974, *Proc. I. A. U. Symp.* **60,** 491.
LO, K. Y., COHEN, M. H., SCHILIZZI, R. T. and ROSS, H. N. : 1977, *Astrophys. J.* **218,** 668.
LO, K. Y., SCHILIZZI, R. T., COHEN, M. H. and ROSS, H. N. : 1975, *Astrophys. J.* **202,** L63.
LOCKMAN, F. J. : 1980, *Astrophys. J.* **241,** 200.
MAIHARA, T., ODA, N., SUGIYAMA, T. and OKUDA, H. : 1978, *Publ. Astron. Soc. Japan* **30,** 1.
MENON, T. K. and CIOTTI, J. E. : *Nature* **227,** 579.
MIRABEL, I. F. : 1976, *Astrophys. Space Sci.* **39,** 415.
MIRABEL, I. F. and FRANCO, M. L. : 1976, *Astrophys. Space Sci.* **42,** 483.
MIRABEL, I. F. and TURNER, K. C. : 1975, *Astrophys. Space Sci.* **38,** 381.
MIRABEL, I. F., PÖPPEL, W. G. L. and VIEIRA, E. G. : 1975, *Astrophys. Space Sci.* **33,** 23.
NADEAU, D., NEUGEBAUER, G., MATTHEWS, K. and GEBALLE, T. R. : 1981, *Astron. J.* **86,** 561.
ODA, N., MAIHARA, T., SUGIYAMA, T. and OKUDA, H. : 1979, *Astron. Astrophys.* **72,** 309.
OKUDA, H., MAIHARA, T., ODA, N. and SUGIYAMA, T. : 1977, *Nature* **265,** 515.
OLNON, F. M., WALTERBOS, R. A. M., HABING, H. J., MATTHEWS, H. E., WINNBERG, A., BRZEZIŃSKA, H. and BAUD, B. : 1981, *Astrophys. J.* **245,** L103.
OORT, J. H. : 1968, *Proc. I. A. U. Symp.* **29,** 41.
OORT, J. H. : 1977, *Annu. Rev. Astron. Astrophys.* **15,** 295.

PAULS, T., DOWNES, D., MEZGER, P. G. and CHURCHWELL, E. : 1976, *Astron. Astrophys.* **46,** 407.
PAULS, T. and MEZGER, P. G. : 1980, *Astron. Astrophys.* **85,** 26.
PÖPPEL, W. G. L. and VIEIRA, E. G. : 1973, *Astron. Astrophys. Suppl. Ser.* **9,** 289.
RADHAKRISHNAN, V., GOSS, W. M., MURRAY, J. D. and BROOKS, J. W. : 1972, *Astrophys. J. Suppl. Ser.* **24,** 49.
RADHAKRISHNAN, V. and SARMA, N. V. G. : 1980, *Astron. Astrophys.* **85,** 249.
RIEKE, G. H., TELESCO, C. M. and HARPER, D. A. : 1978, *Astrophys. J.* **220,** 556.
ROHLFS, K. and BRAUNSFURTH, E. : 1982, *Astron. Astrophys.,* in press.
ROUGOOR, G. W. : 1964, *Bull. Astron. Inst. Netherl.* **17,** 381.
ROUGOOR, G. W. and OORT, J. H. : 1960, *Proc. Nat. Acad. Sci.* **46,** 1.
SANDERS, R. H. and WRIXON, G. T. : 1972a, *Astron. Astrophys.* **18,** 92.
SANDERS, R. H. and WRIXON, G. T. : 1972b, *Astron. Astrophys.* **18,** 467.
SANDERS, R. H. and WRIXON, G. T. : 1973, *Astron. Astrophys.* **26,** 365.
SANDERS, R. H. and WRIXON, G. T. : 1974, *Astron. Astrophys.* **33,** 9.
SANDERS, R. H., WRIXON, G. T. and MEBOLD, U. : 1977, *Astron. Astrophys.* **61,** 329.
SANDERS, R. H., WRIXON, G. T. and PENZIAS, A. A. : 1972, *Astron. Astrophys.* **16,** 322.
SANDQVIST, Aa. : 1972, *Astron. Astrophys. Suppl. Ser.* **9,** 391.
SANDQVIST, Aa. : 1974, *Astron. Astrophys.* **33,** 913.
SARABER, M. J. M. and SHANE, W. W. : 1974, *Astron. Astrophys.* **30,** 365.
SCHWARZ, U., EKERS, R. D. and GOSS, W. M. : 1982, *Astron. Astrophys.,* in press.
SCHWARZ, U., SHAVER, P. A. and EKERS, R. D. : 1977, *Astron. Astrophys.* **54,** 863.
SCOVILLE, N. Z. : 1972, *Astrophys. J. Lett.* **175,** L127.
SCOVILLE, N. Z. : 1980, *Proc. Gregynog Workshop,* 123.
SCOVILLE, N. Z., SOLOMON, P. M. and JEFFERTS, K. B. : 1974, *Astrophys. J. Lett.* **187,** L63.
SCOVILLE, N. Z., SOLOMON, P. M. and PENZIAS, A. A. : 1975, *Astrophys. J.* **201,** 352.
SIMONSON, S. C. and SANCISI, R. : 1973, *Astron. Astrophys. Suppl. Ser.* **10,** 283.
SINHA, R. P. : 1979a, *Astron. Astrophys. Suppl. Ser.* **37,** 403.
SINHA, R. P. : 1979b, Ph.D. Dissertation, University of Maryland.
SINHA, R. P. : 1979c, *Proc. I. A. U. Symp.* **84,** 341.
SOLOMON, P. M., SCOVILLE, N. Z., JEFFERTS, K. B., PENZIAS, A. A. and WILSON, R. W. : 1972, *Astrophys. J.* **178,** 125.
TUVE, M. A. and LUNDSAGER, S. : 1972, *Astron. J.* **77,** 652.
TUVE, M. A. and LUNDSAGER, S. : 1973, *Carnegie Inst. Washington Publ.* No. **630.**
VAN DER KRUIT, P. C. : 1970, *Astron. Astrophys.* **4,** 462.
VAN DER KRUIT, P. C. : 1971, *Astron. Astrophys.* **13,** 405.
VAN WOERDEN, H. : 1970, *Proc. XIV I. A. U. Gen. Assembly* **XIVB,** 217 (Reidel Pub. Co).
VAN WOERDEN, H., ROUGOOR, G. W. and OORT, J. H. : 1957, *C. Rendu* **244,** 1691.
WEAVER, H. and WILLIAMS, D. R. W. : 1973, *Astron. Astrophys. Suppl. Ser.* **8,** 1.
WESTERHOUT, G. : 1973, *Maryland-Green Bank Galactic 21-cm Line Survey,* University of Maryland, College Park.
WHITEOAK, J. B. and GARDNER, F. F. : 1978, *Proc. Astron. Soc. Aust.* **3,** 266.
WHITEOAK, J. B. and GARDNER, F. F. : 1979, *Mon. Not. R. Astron. Soc.* **188,** 445.
WHITEOAK, J. B., ROGSTAD, D. H. and LOCKHART, I. A. : 1974, *Astron. Astrophys.* **36,** 245.
WILLIAMS, D. R. W. : 1973, *Astron. Astrophys. Suppl. Ser.* **8,** 505.
WILLNER, S. P. : 1978, *Astrophys. J.* **219,** 870.
WOLLMAN, E. R., GEBALLE, T. R., LACY, J. H., TOWNES, C. H. and RANK, D. M. : 1976, *Astrophys. J.* **205,** L5.
WRIXON, G. T. and SANDERS, R. H. : 1973, *Astron. Astrophys. Suppl. Ser.* **11,** 339.
ZUCKERMAN, B. and KUIPER, T. B. H. : 1980, *Astrophys. J.* **235,** 840.

(This Page Intentionally Left Blank)

TABLE I. — *Summary of survey observations of the nuclear region of the Galaxy.*

I. Observations of HI λ21 cm Line

Reference	Telescope	ℓ-coverage (degrees)	b-coverage (degrees)	v-coverage (km s^{-1})	Beam (arc min)
Rougoor, 1964	Dwingeloo 25-m	352 to 22, Δℓ=0.5	-0.6 to 0.9, Δb=0.25	|v| ∿ 50 to 275, Δv=9.4 or 4.2	36
Kerr & Vallak, 1967	Parkes 210-foot	359 to 1, Δℓ=0.1	-1 to 1, Δb=0.1	-165 to 165, Δv=7	15
Cugnon, 1968	Dwingeloo 25-m	346 to 356, Δℓ=1.0	1 to 7, Δb=1.0	-50 to 150, Δv=3.4	36
Kerr, 1969	Parkes 210-foot	300 to 60, Δℓ=1.0	-2 to 2, Δb=0.2	-250 to 250, Δv=7	15
Burton, 1970	Dwingeloo 25-m	354 to 120, Δℓ=0.5	b=0 only	center vel.±270, Δv=1.7	36
Kerr & Hindman, 1970	Parkes 210-foot	185 to 63, Δℓ=1.0	b=0 only	-250 to 250, Δv=7.0	15
Menon & Ciotti, 1970	Green Bank 140-foot	350 to 16, Δℓ=0.4	b=0.3, -0.06, -0.4	center vel.±264, Δv=1.7	21
van der Kruit, 1970	Dwingeloo 25-m	350 to 10, Δℓ=1.0	-5 to 5, Δb=1.0	|v| ∿ 75 to 300, Δv=10.5	36
Sanders & Wrixon, 1972a, & Sanders et al., 1972	Bell Labs 6-m horn	350 to 12, Δℓ=2	-10 to 0, Δb=2	-340 to -40, Δv=16	150
Sanders & Wrixon, 1972b	Bell Labs 6-m horn	355 to 5, Δℓ=2	-5 to 5, Δb=2	-300 to 300, Δv=16	150
Simonson & Sancisi, 1973	Dwingeloo 25-m	356 to 24, Δℓ=0.5	varies; in core 0 to 5, Δb=0.5	-120 to 120, Δv=3.4	36
Tuve & Lundsager, 1973	DTM 60-foot	336 to 270, Δℓ=4.0	-16 to 16, Δb=1 or 2	center vel.±100, Δv=4	47
Westerhout, 1973	Green Bank 300-foot	13 to 235, Δδ=0.1	-2 to 2, Δb=0.2	center vel.±120, Δv=2	12
Wrixon & Sanders, 1973	Green Bank 140-foot	357 to 3, Δℓ=0.3	-3 to 3, Δb=1	-300 to 300, Δv=5.5	21
Lindblad, 1974	Green Bank 140-foot	339 to 12, Δℓ=3.0	-10 to 15, Δb=0.3	-120 to 120, Δv=1	21
Saraber & Shane, 1974	Dwingeloo 25-m	7 to 10, Δℓ=0.5	-7 to -2, Δb=0.5	-300 to -70, Δv=3.4	36
Cohen, 1975	Jodrell Bank MkII	355 to 10, Δℓ=1.0	-5 to 5, Δb=0.25	-300 to 300, Δv=7.3	33
Mirabel, Pöppel, & Vieira, 1975	IAR 30-m	332 to 354, Δℓ=1.0	1 to 7, Δb=1.0	-100 to 100, Δv=2	30
Mirabel & Turner, 1975	IAR 30-m	irregular near ℓ,b= 355, -12		-70 to 130, Δv=4	30
Mirabel, 1976	IAR 30-m	335 to 5, Δℓ=1	-5 to 5, Δb=1.1	-1000 to -300, Δv=25	30
Mirabel & Franco, 1976	IAR 30-m	6 to 10, Δℓ≤1.0	-7 to -2, Δb≤1	-130 to -310, Δv=25(2)	30
Westerhout, 1976	Effelsberg 100-m	358 to 250, Δℓ=0.2	b=0 only	center vel.±200, Δv=2	9(12)
Burton, Gallagher, & McGrath, 1977	Green Bank 140-foot	349 to 12, Δℓ=1.0	-10 to 10, Δb=1	-500 to 500, Δv=5.5	21
Sanders, Wrixon, & Mebold, 1977	Effelsberg 100-m	357 to 3, Δℓ=0.1	b=0 only	-300 to 300, Δv=2.8	9
Cohen & Davies, 1979	Jodrell Bank MkIA	359 to 1, Δℓ=0.5	-1 to 1, Δb=0.2	-300 to 300, Δv=7.3	13
Sinha, 1979a	Green Bank 140-foot	339 to 11, Δℓ=0.5	-2 to 2, Δb=0.25	center vel.±210, Δv=5.0	21
Braunsfurth & Rohlfs, 1981	Effelsberg 100-m	358.5 to 1.5, Δℓ=0.15	-1.5 to 1.5, Δb=0.15	-300 to 300, Δv=3.0 & 6.0	9
Kerr, Bowers & Henderson, 1981	Parkes 210-foot	230 to 350 at b=0 Δℓ=0.1	-2 to 2 at Δℓ=1, Δb=0.1	center vel.±160, Δv=2	16
this paper	Green Bank 140-foot	349 to 13, Δℓ=0.5	-10 to 10, Δb=0.5	-340 to 340, Δv=5.5	21

Sensitivity (K)	Form of Display	Special Characteristics and Particular Uses
2.5	$(\ell v)\|_b$ & $(b,v)\|_\ell$	Pioneering HI investigation of nucleus. This observing program led to discovery of absorption of Sgr A emission by HI in the 3-kpc arm, and of the expanding motion of this arm (see van Woerden, Rougoor, and Oort; Rougoor and Oort).
3.0	$(b,v)\|_\ell$	Systematic coverage of inner 4 square degrees; interpretation distinguishes most intense emission and absorption features.
2.0	special purpose	Observations made for a study of the forbidden-velocity feature near $\ell,b,v=349^\circ,3^\circ,50$ km s^{-1}.
3.0	$(\ell,v)\|_b$ & $(b,v)\|_\ell$	First systematic survey of southern galactic equator; complementary to Westerhout's (1973) Maryland-Green Bank survey.
2.0	$(\ell,v)\|_b$ & spectra	Galactic equator only; interpretation (Burton 1971) in terms of general galactic kenematics, not specific to nucleus.
3.0	$(\ell,v)\|_b$	Systematic coverage of southern galactic equator.
2.0	special purpose	Observations used for study of two features with low, non-zero (-27 km s^{-1} and -14 km s^{-1}) velocities at the $\ell=0^\circ$ crossing, interpreted as expanding arms.
0.5	$(b,v)\|_\ell$, some $(b,v)\|_v$	Systematic coverage of extreme velocities, on a relatively coarse grid. Interpretation stresses individual features and their possible expulsion from the galactic nucleus; see van der Kruit, 1971.
0.1	special purpose	Observations of the "g"-feature prominent near $b=0^\circ\rightarrow-4^\circ$, v -160 km s^{-1}, and interpretation of this feature in terms of an expanding, rotating gas ring.
0.1	special purpose	Observations and interpretation of anomalous emission in opposed quadrants; association drawn with the λ20 cm continuum ridges of Kerr and Sinclair (1966).
2.0	spectra; $(\ell,v)\|_b$ & $(b,v)\|_\ell$	Survey only; interpretation in d'Odorico, Sancisi, and Simonson (1969) emphasizes HI self-absorption across the central region and two emission features near $\ell,b,v=-1^\circ.5$, $4^\circ.5$, -36 km s^{-1} and $-3^\circ.5$, $2^\circ.0$, -20 km s^{-1}.
2.0	spectra & gaussian decomposition	Interpretation, in Tuve and Lundsager (1972) in terms of general galactic kinematics, not specific to nucleus
2.0	$(\ell,v)\|_b$	Systematic coverage of northern galactic equator; complementary to Kerr, Bowers, and Henderson's (1981) Parkes survey.
0.2	$(\ell,v)\|_b$	Detailed latitude strips at good sensitivity. Survey only; the interpretation in Sanders and Wrixon (1973) discusses the gas density in the inner 500 pc, and apparent symmetries in the HI kinematics and distribution.
2.0	$(b,v)\|_\ell$	High-velocity-resolution data with detailed coverage in latitude; survey only.
0.6	special purpose	Observations and interpretation of Shane's isolated, anomalous-velocity feature near $\ell,b,v=8^\circ$, -4°, 212 km s^{-1}.
0.3	$(b,v)\|_\ell$	Systematic coverage, with good latitude detail. The survey paper contains substantial discussion with emphasis on specific emission features; additional interpretation in Cohen and Davies (1976), and in Cohen and Davies (1979).
2.0	special purpose	Observations made for a study of Cugnon's feature, near $\ell,b,v=349^\circ,3^\circ,50$ km s^{-1}.
2.0	special purpose	Observations and interpretation of extended anomalous-velocity structure most intense near ℓ,b, $v=355^\circ$, -12°, +45 km s^{-1}.
0.3	none	Very broad kinematic-coverage at negative velocities, revealing no emission beyond the usual galactic kinematic boundary (cf. Burton, Gallagher, and McGrath).
0.2	special purpose	Observations made for a study of Shane's feature near $\ell,b,v=8^\circ,-4^\circ$, 212 km s^{-1}.
0.4	$(\ell,v)\|_b$	Highest angular-resolution HI map of galactic equator; smoothed to resolution of 300-foot telescope for comparison with Maryland-Green Bank survey. Unpublished, but available in several forms.
0.2	$(b,v)\|_\ell$	Broad angular coverage on a moderately coarse grid; broad velocity coverage. Survey only; interpretation in Burton and Liszt (1978).
0.5	$(\ell,v)\|_b$	High-angular-resolution at $b=0^\circ$. Interpretation in terms of a spiral enhancement of gas density in a purely rotating disk.
0.5	$(\ell,v)\|_b$ & $(b,v)\|_\ell$	High-angular-resolution data within 1° of galactic center. Interpretation stresses non-circular motions and the tilted nature of the gas distribution.
0.2	$(\ell,v)\|_b$ & $(b,v)\|_\ell$	Systematic coverage; broad in ℓ on a moderately dense grid, less broad in b but on a denser grid. Survey only; interpretation in Sinha (1979b).
2.5	$(\ell,v)\|_b$, $(b,v)\|_\ell$ & $(\ell,b)\|_v$	High-angular-resolution data on a dense grid in the galactic core, but very low sensitivity.
2.0	$(\ell,v)\|_b$ & $(b,v)\|_\ell$	Systematic coverage of southern galactic equator; complementary to Westerhout's (1973) Maryland-Green Bank survey.
0.1	$(\ell,v)\|_b$, $(b,v)\|_\ell$ & $(\ell,b)\|_v$	Systematic, broad coverage in angle and velocity on a moderately dense grid; good sensitivity. Survey only; interpretation in Liszt and Burton (1980).

TABLE II. — *Observations of CO emission.*

Reference	Telescope	Source	Wavelength/Freq.	Beam
Solomon et al., 1972	NRAO 36-foot	^{12}CO: J=1 → 0	2.6mm	65"
Sanders & Wrixon, 1974	NRAO 36-foot	^{12}CO: J=1 → 0	2.6mm	65"
Scoville, Solomon, & Jefferts, 1974	MWO 16-foot	^{12}CO: J=1 → 0	2.6mm	2'
Liszt, Sanders, & Burton, 1975	NRAO 36-foot	^{12}CO: J=1 → 0	2.6mm	65"
Scoville, Solomon, & Penzias, 1975	NRAO 36-foot & 140-foot	^{12}CO, ^{13}CO, CS, & H_2CO	-	∿1' & 2'
Bania, 1977	NRAO 36-foot	^{12}CO: J=1 → 0	2.6mm	65"
Liszt et al., 1977	NRAO 36-foot	^{12}CO: J=1 → 0	2.6mm	65"
Liszt & Burton, 1978	NRAO 36-foot	^{12}CO: J=1 → 0	2.6mm	65"
Bania, 1980	NRAO 36-foot	^{12}CO: J=1 → 0	2.6mm	65"
Inatani, 1980	KTC 1.5-m	^{12}CO: J=1 → 0	2.6mm	10'
Scoville, 1980	NRAO 36-foot	^{12}CO & ^{13}CO	2.6mm	65"
Burton and Liszt, 1981	NRAO 36-foot	^{13}CO: J=1 → 0	2.7mm	68"
Liszt and Burton, 1982	NRAO 36-foot	^{12}CO: J=1 → 0	2.6mm	65"

Sky Coverage	Special Characteristics and Particular Uses
$(\ell,v)\|_b$ map at b=-2' from ℓ = 359°.7 to 2°.8	Early ℓ-cut through Sgr molecular complex; additional interpretation in Scoville (1972) in terms of an "expanding molecular ring".
20' longitude strip at b=0'	Early identification of bright molecular emission components in nucleus.
$(\ell,v)\|_b$ map at b=0°, $\|\ell\| < 3°$, $\Delta\ell$ = 10'	Early large-scale ℓ,v map of CO emission near galactic equator. Interpretation emphasizes kinematic models based on expanding, rotating spiral structures.
Dense grid of limited extent centered on Sgr A West	Preliminary survey of CO in Sgr A molecular-cloud complex; identification of CO self-absorption features.
Position-velocity maps of some 20' length through Sgr B2 cloud	Interpretation emphasizes derivation of densities in Sgr B2 cloud and identification of complex motions within it.
Large-scale $(\ell,v)\|_b$ map at b=0° from ℓ = 352° to 10°; $(b,v)\|_\ell$ cuts at ℓ = 7.5 and 359°.18	Observations directed toward large-scale CO emission features near the galactic equator, especially the 3-kpc arm and nuclear disk; interpretation involves considerations of resonance orbits, kinematic rings, and explosions in galactic nucleus.
Representative observations of inner 2° of ℓ at b=-7', -5', -1', and +1'	Identification of several large-scale anomalous CO features with HI counterparts; discussion of CO absorption features (see also Zuckerman and Kuiper, 1980 and Linke, Stark, and Frerking, 1980).
ℓ = -23' to 145' at b=-3'; constant-position strips at b=-63' and 57', and at ℓ = 117', 47', -3', and -123'.	Interpretation emphasizes evidence for tilted gas distribution; additional discussion of the "expanding molecular ring" and of total gas density in the gas.
$(\ell,v)\|_b$ maps at b=±20' and 0' from =350° to 25° at $\Delta\ell$=0°.5; $(b,v)\|_\ell$ maps at ℓ=23°.5 and 355° from b=-1° to 1°.	Extensive longitude scans at several latitudes used for study of 3-kpc arm and the +135 km s^{-1} feature; proton mass of inner galaxy discussed.
ℓ = 0°.4 to 1°.8, $\|b\| \leq 0°.4$, on a 0°.2 grid	Two-dimensional study of intense CO emission (mostly residing at positive velocities), noting gradients in velocity and position.
$(\delta,v)\|_\alpha$ maps through Sgr B2; $(b,v)\|_\ell$ maps at ℓ=0°,±1°.	CO data interpreted in the context of molecular gas in the galaxy.
$(\ell,v)\|_b$ map at b=-3' from ℓ = -82' to 74', $\Delta\ell$ = 2'.	Synoptic map of emission from the ^{13}CO isotope along latitude of Sgr A.
$(\ell,b)\|_v$ maps covering -34'<ℓ<50', -16'<b<28', at $\Delta\ell$,Δb=2'	Two dimensional mapping of Sgr molecular complex and an anomalous tilted structure.

TABLE III. — *Observations of lines other than HI and CO.*

Reference	Telescope	Line	Wavelength/Freq.	Beam
Sandqvist, 1972 & 1974	Green Bank 140-foot & moon	HI, OH, H_2CO	21, 18, 6 cm	$\lesssim$1'
Cohen & Few, 1976	Jodrell Bank MkIa	OH abs.	1665 & 1667 MHz	11'
Wollman et al., 1976	CTIO 1.5m & Lick 3-m	NeII	12μm	8"
Fukui et al., 1977	Tokyo 6-m	HCN:J=1 0	3.4 mm	2'
Whiteoak & Gardner, 1978	Parkes 64-m	H_2CO abs.	4.8 GHz	4!4
Baud et al., 1979	Dwingeloo, Effelsberg & Green Bank	OH masers	1612 MHz	31,8',18'
Lacy et al., 1979	Las Campanas 2.5-m	NeII	12μm	3"5
Whiteoak & Gardner, 1979	Parkes 64-m	H_2CO abs.	6 cm	4!4
Fukui et al., 1980	Tokyo 6-m	HCO^+: J=1 0	3.4 mm	2'
Güsten & Downes, 1980 Bieging et al., 1980	Effelsberg 100-m	H_2CO abs.	4.8 GHz	2!6
Lacy et al., 1980	Las Campanas 2.5-m	NeII	12μm	3"5
Lockman, 1980	Green Bank 140-foot	H166α	1.425 GHz	21'
Pauls & Mezger, 1980	Effelsberg 100-m	H109α	5 GHz	2!6
Cohen & Few, 1981	Jodrell Bank MkII	H_2CO abs.	6 cm	10'x9'
Linke et al., 1981	Bell Labs 7-m	HCO^+ et al.	3.4 mm	2'
Nadeau et al., 1981	Las Campanas 2.5-m	Bγ	2.2μm	5"
Olnon et al., 1981	Effelsberg 100-m	OH	1612 MHz	8'

Sky Coverage	Special Characteristics and Particular Uses
Lunar-occultation data of region covering about 1 square degree near the Sgr A complex.	High angular-resolution study with particular emphasis on absorption feature at +40 km s^{-1}.
$(\ell,v)\|_b$ and $(b,v)\|_b$ maps at $\ell=358^\circ$ to 3°, $\|b\|\lesssim 0\overset{\circ}{.}6$, on $0\overset{\circ}{.}2$ grid; $\Delta v=6.1$ km s^{-1}.	Complements HI surveys, especially Cohen (1975). Interpretation discusses possible evidence for a central bar and for explosive events in the nucleus.
Positions near Sgr A West.	Data reveal systematic motions with respect to massive stellar component, and provide an upper limit for mass within 0.8 pc of center. (See Aitken et al., 1974).
Two-dimensional data on a 2' grid of region $\ell\sim -10'$ to 40', $b\sim -10'$ to 5'.	Interpretation directed toward Sgr A complex, and includes discussions of the possibility of ejection of the Sgr A and 32 clouds from the nucleus.
Two-dimensional data covering some 200 square minutes in neighborhood of Sgr A. High velocity resolution of 0.24 km s^{-1}.	High velocity-resolution reveals new low-velocity absorption features which the authors associate with the galactic nucleus.
Systematic survey of about 20 square degrees made with varying grids and sensitivity; generally $\ell>358^\circ$, $\|b\|<2^\circ$.	Catalogue of Type II OH/12 emission sources. Interpretation in Baud et al. (1981) includes discussion of selection effects, projected surface density of sources, evidence for a nuclear bulge, and kinematics of the sample.
5" grid near SgrA West, $\Delta v=36$ km s^{-1}.	Complex array of small sources mapped in inner 20"; the clouds appear to be rotating about an axis tilted strongly from that of galactic rotation.
$\ell=358\overset{\circ}{.}6$ to $2\overset{\circ}{.}8$, $b=-0\overset{\circ}{.}2$ to $+0\overset{\circ}{.}1$, $\Delta v=2.4$ km s^{-1} at $-26<v<360$ km s^{-1}.	General survey of H_2CO absorption and line/continuum data. Interpretation of individual features.
19 positions in Sgr A and B2 mostly lying near the tilted "straight ridge" feature of Fukui et al. (1977)	Compares HC_{O^+}, HCN, and CO data from Sgr A and B2 clouds, and from self-absorption absorption features near 0 km s^{-1}.
Fully sampled observations of inner 300 pc: $\|b\|\lesssim 0\overset{\circ}{.}2$, $\|\ell\|\lesssim 0\overset{\circ}{.}4$; $\|v\|\lesssim 310$ km s^{-1}, $\Delta v=2.0$ km s^{-1}.	Detailed interpretation includes discussion of Sgr A clouds, cloud at +40 km s^{-1}, nuclear disk, and expanding molecular ring. Observations of HCN, CO and radio continuum incorporated in the analysis.
Some 60-odd spectra measured in a ~3" grid centered on Sgr A West.	Data reveal that the ionized gas within Sgr A is clumped into clouds with diameters 0.1-0.5 kpc, velocity dispersions 100 km s^{-1}, and high systematic velocities. Interpretation includes discussion of cloud generation and dissipation at a rate of few per 10^3 yr.
At $b=0^\circ$, spectra every degree from $\ell=350^\circ$ to 15°, at $b=\pm 0\overset{\circ}{.}33$, every 4° from $\ell=350^\circ$ to 14°.	Data show a low star-formation rate in the 3-kpc arm and, in general, in the molecular features in the core. Comparison with OH maser, CO, and HI data.
32 positions superimposed on the arc-like continuum source	Maps of spectral emission from region of arc-like source; emission strongest near $v\sim -40$ km s^{-1}.
$\ell=358^\circ$ to 5°, $b=-0\overset{\circ}{.}5$ to $+0\overset{\circ}{.}5$, $\Delta v=2.1$ km s^{-1}.	General, detailed survey. Interpretation in terms of radial distribution and structure of individual features.
HCO^+: $\ell=-1\overset{\circ}{.}6$ to $+2\overset{\circ}{.}0$ at $b=-0\overset{\circ}{.}05$. Spectra of other molecules toward Sgr B2.	Map of HCO^+ distribution. Absorption features in several species yield column densities and large total mass.
10 positions near center, $\Delta v=85$ km s^{-1}.	Bγ recombination line of H shows spectra similar to those of Ne II line and confirms ionized gas in discrete clouds.
$\ell=358^\circ$ to 15°, $\|b\|\lesssim 1\overset{\circ}{.}3$.	Discussion of distribution in galactic coordinates and radial velocity of 57 OH/IR sources.

TABLE IV. — *Observations of infrared continuum emission.*

Reference	Telescope	Wavelength/Freq.	Beam
Becklin & Neugebauer, 1968	24, 60, and 200 in	1.7, 2.2, 3.4μm	0!8 to 1!8
Hoffmann, Frederick, & Emery, 1971	12 in (balloon)	100±50μm	6'
Becklin & Neugebauer, 1975	Hale 200 in	2.2, 10μm	2"5 & 2"3
Harvey, Campbell, & Hoffmann, 1976	90 cm (KAO)	53, 100, 175μm	17" & 30"
Ito, Matsumoto, & Uyama, 1977	10 cm (balloon)	2.4μm	2°
Okuda et al., 1977	20 cm (balloon)	2.4μm	1°
Becklin et al., 1978	Hale 200 in	1.2 to 13μm	2"3
Hildebrand et al., 1978	CTIO 4-m	540μm	∿100"
Hofmann, Lemke, & Frey, 1978	15 cm (balloon)	2.5μm	1°
Mahaira et al., 1978	20 cm (balloon)	2.4μm	1°
Rieke, Telesco, & Harper, 1978	various	10-56μm	2"-3'
Hayakawa et al., 1979	10 cm (balloon)	2.4μm	1°.7
Oda et al., 1979	20 cm (balloon)	2.4μm	0°.6
Harris, Lemke, & Hofmann, 1980	15 cm (balloon)	2.4μm	1°.1
Hayakawa et al., 1981	10 cm (balloon)	2.4μm	

TABLE V. — *Observations of radio continuum emission.*

Reference	Telescope	Wavelength/Freq.	Beam
Downes & Maxwell, 1966	Haystack 120-foot	3.75 cm	4!2
Kerr & Sinclair, 1966	Parkes 210-foot	20 cm	14'
Altenhoff et al., 1970	Green Bank 140-foot	11 cm	11'
Pauls et al., 1976	Effelsberg 100-m	2.8 cm	1!3
Downes et al., 1978	Westerbork SRT Effelsberg 100-m	5 GHz 4.9 & 10.7 GHz	∿6"x40" 2!6 & 1!3
Altenhoff et al., 1979	Effelsberg 100-m	4.9 GHz	2!6

Sky Coverage	Special Characteristics and Particular Uses
central 60 pc	Pioneering observations and analysis of infrared radiation from galactic nucleus; comparison with radio data from Sgr A and with IR from nucleus of M31.
$\ell=358^\circ$ to 2°, $\lvert b\rvert \leq 1^\circ$	Far-IF observations of general region of Sgr source; analysis in terms of thermal dust emission model.
central 1'	Photometric IR maps of central 1' of the galactic core, resolved into siacrete sources plus an extended ridge of emission.
central 3'	Far-IF observations of dust temperatures near Sgr A.
$\ell=353^\circ$ to 35°, $\lvert b\rvert < 15^\circ$	IR survey of nuclear bulge region.
$\ell=350^\circ$ to 30°, $\lvert b\rvert < 15$	IR survey of nuclear bulge region.
central 40'	Photometry from 1.2 to 12μm (and spectrophotometry from 8 to 13μm; see Willner, 1978) of compact stellar galactic center sources.
15'x15' region surrounding Sgr A.	Sub mm data revealing ridge parallel to equator but not peaked at Sgr A.
10° x 15° region near center	Near-IR survey of bulge region.
$\ell=350^\circ$ to 30°, $\lvert b\rvert < 15^\circ$	Details of experiment of Okuda et al. (1977); interpretation yielding models of galactic dust distribution.
Maps of inner few arcmin	Mid- and long-wavelength IR maps of central region, studying scales from 0.07 pc to 9 pc.
$\ell=290^\circ$ to 20°, $\lvert b\rvert \lesssim 8^\circ$	IR surface brightness of southern galactic plane; IR emission displays asymmetries shown by HI data.
$\ell=348^\circ$ to 32°, $\lvert b\rvert \lesssim 10^\circ$	Discussion centers on distortions to bulge caused by interstellar dust, and on the anomalous source at $\ell=355^\circ$, $b=-1^\circ$.
$\ell=352^\circ$ to 8° at $b=0^\circ$	IR profile compared with Bania's (1977) CO emission; used to estimate mass-to-luminosity ratio of central bulge.
$\ell=290^\circ$ to 50°, $\lvert b\rvert \leq 7^\circ$	Near-IR survey of the galactic plane. Analysis stresses morphological properties of galactic disk.

Sky Coverage	Special Characteristics and Particular Uses
region within 1° of Sgr A.	Survey of thermal radiation around galactic center, revealing substantial structure for the first time.
$\ell=355^\circ$ to 5°, $\lvert b\rvert \lesssim 1^\circ.5$.	Description of a symmetrical pattern of ridges of emission appearing in opposed galactic quadrants and suggestive of a pair.
$\ell=335^\circ$ to 75°, $\lvert b\rvert \lesssim 2^\circ$.	General survey of nonthermal continuum emission. Surveys at 1.4 and 5 GHz included in reference.
region within 15' of Sgr A.	Observations of thermal radiation especially from Sgr A and the Arc structure.
coverage of continuum sources in the general region $\lvert\ell\rvert<2^\circ$, $\lvert b\rvert<1^\circ$.	Catalogue of 74 compact radio continuum sources in the central few degress, with detailed phenomenological discussion of most prominent sources.
systematic survey of galactic disk, $\ell=357^\circ.5$ to 60°, $\lvert b\rvert \leq 1^\circ$.	General survey of galactic equator region at high resolution.

TABLE VI. — *Interferometric observations.*

Reference	Interferometer	Wavelength/Freq.	Beam
Radhakrishnan et al., 1972	Parkes	21-cm HI abs.	∿10'; $\Delta v \sim 2$ km s^{-1}
Balick & Brown, 1974	Green Bank	2.7 & 8.1 GHz	spacings 3-8.5x10$^5\lambda$
Balick & Sanders, 1974	Green Bank	2.7 & 8.1 GHz	2"
Little, 1974	Molonglo Cross	75 cm	2!9
Whiteoak, Rogstad, & Lockhart, 1974	Owens Valley	6 cm H_2CO abs.	20"x40"; Δv=3.1 km s^{-1}
Ekers et al., 1975	Westerbork & Owens Valley	5 GHz	6"x34"
Lo et al., 1975	VLBI	3.7 cm	spacings 3.6-4.4x10$^6\lambda$
Bieging, 1976	Owens Valley	1667 MHz OH abs.	3!3; Δv=1.4 km s^{-1}
Davies, Walsh, & Booth, 1976	Jodrell Bank	0.4, 1.0, & 1.7 GHz	spacings 3-13x10$^4\lambda$
Lo et al., 1977	VLBI	3.7 cm	spacings 10^6 to 10^8
Kellermann et al., 1977	VLBI	7.8 GHz	spacings 15-10x10$^6\lambda$
Schwarz, Shaver, & Ebers, 1977	Westerbork	21-cm HI abs.	25"x120"; $\Delta v \sim 20$ km s^{-1}
Brown, Lo, & Johnston, 1978	Green Bank & VLA	1.3-11.1 cm	
Brown, Johnston, & Lo, 1981	VLA	6 cm	0!7
Schwarz, Ekers, & Goss 1982	Westerbork	21 cm HI abs.	23"x143"; Δv=4.1 km s^{-1}
Ekers & Schwarz, 1982	VLA	20 cm & 6 cm	2" - 10"
Liszt et al., 1982	VLA	21 cm HI abs.	12"x12"; Δv=5.2 km s^{-1}

Sky Coverage	Special Characteristics and Particular Uses
Sgr A	Interpretation of simple absorption spectrum emphasizes prominence of feature at +50 km s^{-1}.
Sgr A	Detection of sub-arcsecond structure in inner core of galactic nucleus.
Sgr A & Sgr B.	Maps of radio fine structure discussed in terms of physical conditions near the center.
region within 1^{o} of Sgr A.	Detailed map of long wavelength continuum structure.
Sgr A East & West.	Interpretation of +50 km s^{-1} feature (which disappears moving from East to West) suggests passage of a cloud between two continuum sources.
Sgr A East & West	"WORST" map of two major components of Sgr A, made with full synthesis given resolution corresponding to 0.3x1.7 pc.
Sgr A East	VLBI observations revealing at λ3.7 cm a source of linear size $\lesssim$200 au.
Region of Sgr A & Sgr B	Observations and interpretation of absorption by discrete OH condensations against Sgr A and B2, at $-200<v>100$ km s^{-1}.
Sgr A	Interpretation emphasizes influence of interstellar scattering, and suggests supernova remnant or pulsar as central source.
Sgr A East	VLBI observations at 3.7cm which indicate that the nonthermal compact source has a linear size of ∿140 au and a total flux density of 0.9 Jy (1967?).
Sgr A East	VLBI observations at 7.8 GHz showing that the compact radio source in the galactic center has dimensions $\lesssim$200 au and a core containing 25% of the 7.8 GHz emission of ∿10 au extent.
Region of Sgr A	Observations and interpretation absorption by HI in front of Sgr A, at $\lvert v\rvert \lesssim 150$ km s^{-1}.
Sgr A East	Multifrequency observations which show that flux density of compact source increases with increasing frequency for ν<25 GHz ($\propto \nu^{0.5}$).
Sgr A West	Map of Sgr A West shows trunk-like structure of thermal emission around the compact source; comparison with 10μ IR data.
Sgr A East & West	Gaussian analysis used to constrain abundance of high-dispersion ($\Delta_v \sim 35$ km s^{-1}) ISM HI suggested by Radhakrishnan and Sarma (1980).
Sgr A East & West	Observations show that Sgr A East is part of a full shell passing through West; spectral index map distinguishes thermal and non-thermal emission.
Sgr A East & West	HI absorption map of inner 4'. Comparison with detailed map of CO emission shows that many of the HI features have extended molecular counterparts.

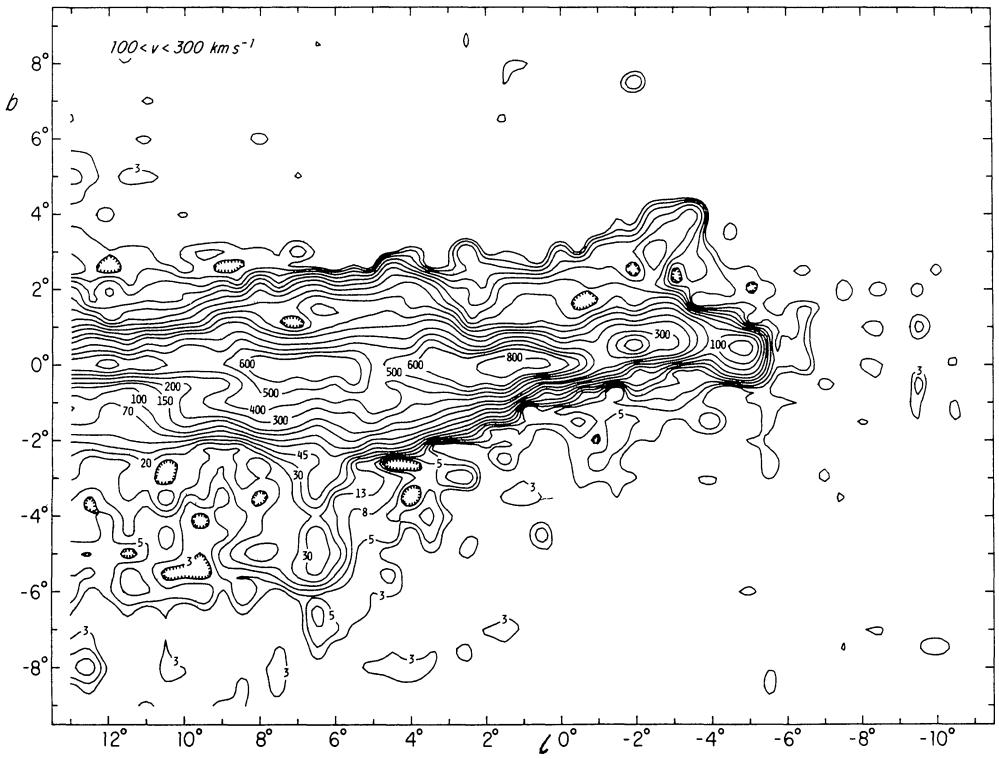

FIGURE 1a. — Contours of observed HI antenna temperature integrated over the velocity range $+ 100 < v < + 300$ km.s^{-1} and projected onto the plane of the sky. Material in this velocity range is « forbidden », at $l < 0°$, in terms of circular differential galactic rotation. The contours are labelled in units of K.km.s^{-1}. At a distance of 10 kpc, a contour level 100 K.km.s^{-1} over a solid angle of one square degree corresponds to $6.3 \times 10^4 M_\odot$ of HI if, as seems plausible, the gas is optically thin.

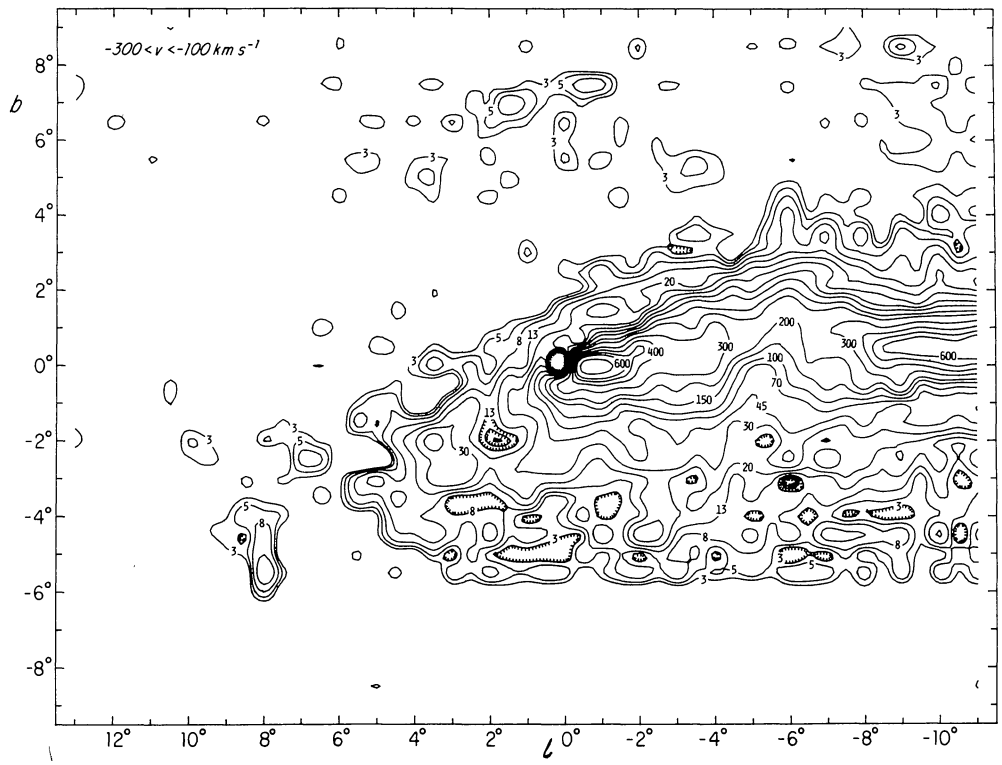

FIGURE 1b. — Contours of observed HI antenna temperature integrated over the velocity range $- 300 < v < - 100$ km.s^{-1} and projected onto the plane of the sky. Material in this velocity range is « forbidden », at $l > 0°$, in terms of circular differential galactic rotation. The contours are labelled in units of K.km.s^{-1}.

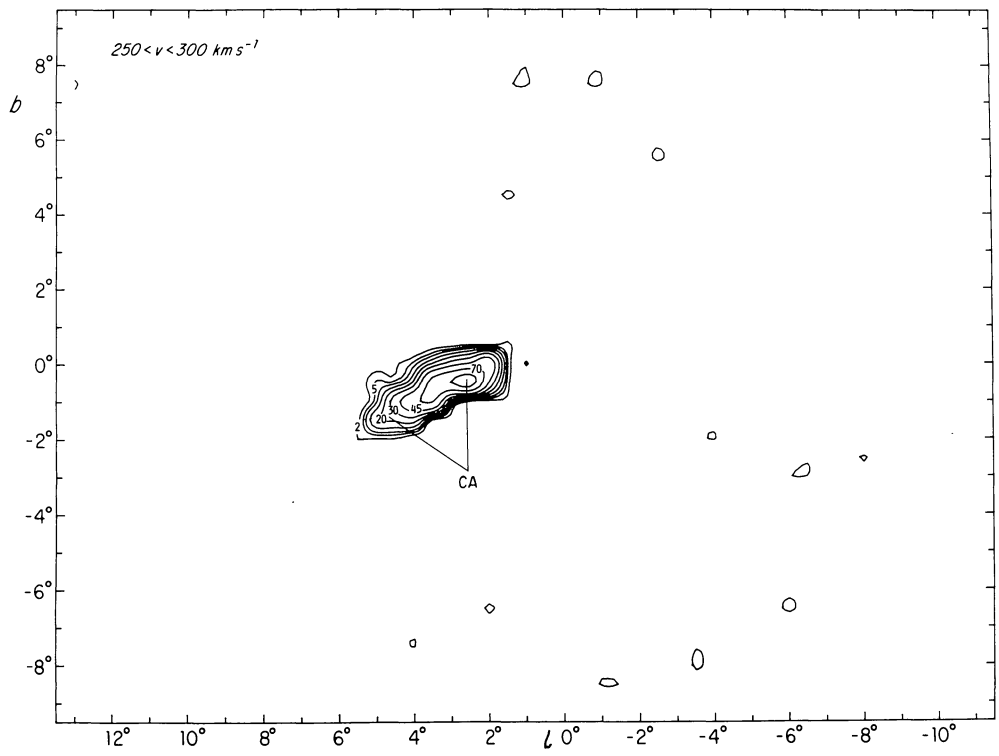

FIGURE 2a. — Map on the plane of the sky of observed HI antenna temperature integrated over the velocity range $250 < v < 300$ km.s^{-1}. Emission in this velocity range has been attributed to the connecting arm feature discussed by Rougoor (1964).

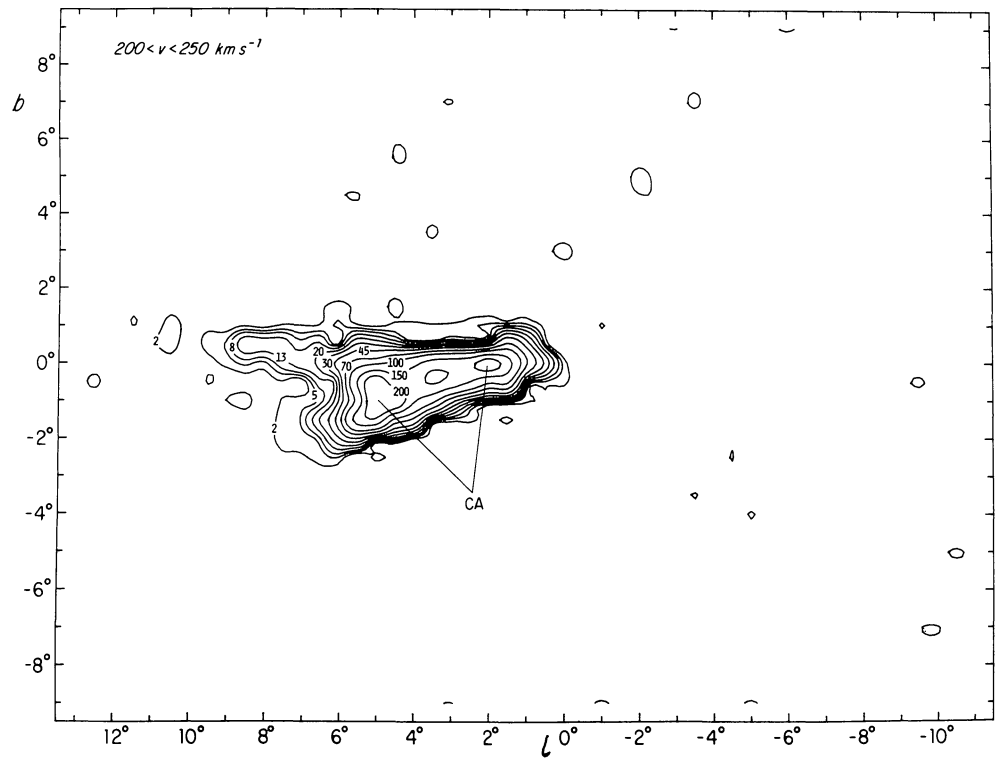

FIGURE 2b. — Map on the plane of the sky of observed HI antenna temperature integrated over the velocity range $200 < v < 250$ km.s^{-1}. The emission labelled CA corresponds to the connecting arm feature.

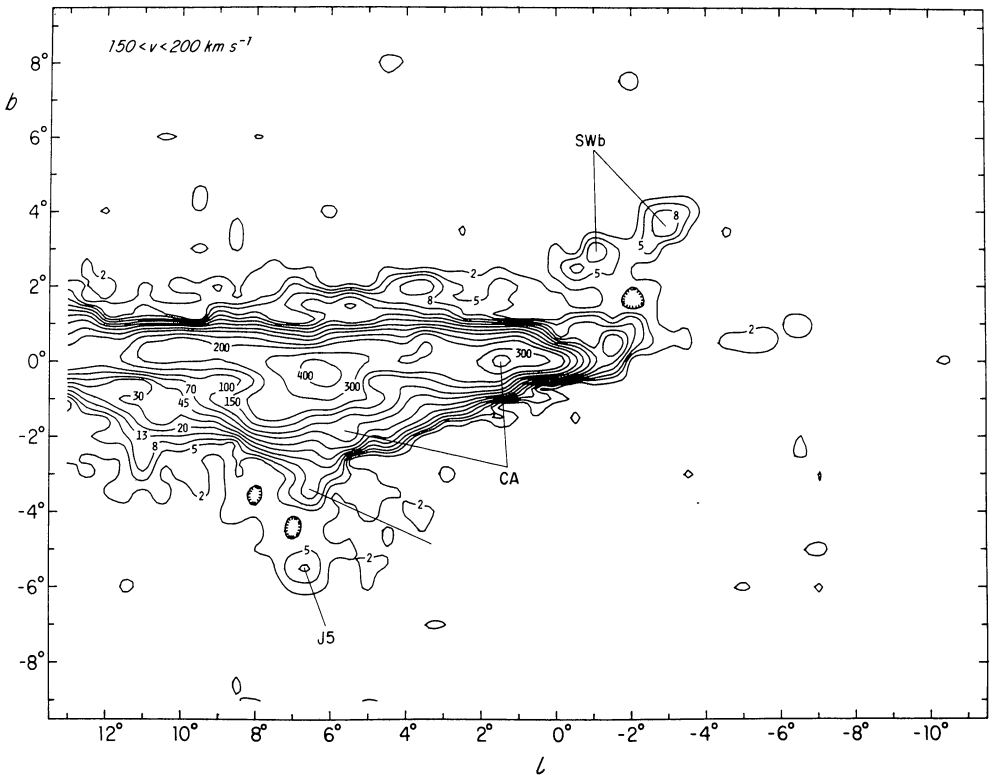

FIGURE 2c. — Map on the plane of the sky of observed HI antenna temperature integrated over the velocity range $150 < v < 200$ km.s^{-1}. The locations of emission are labelled for the feature SWb (Sanders and Wrixon, 1972b), corresponding to feature J2 of Cohen (1975), for the connecting arm feature CA, and for feature J5 of Cohen (1975).

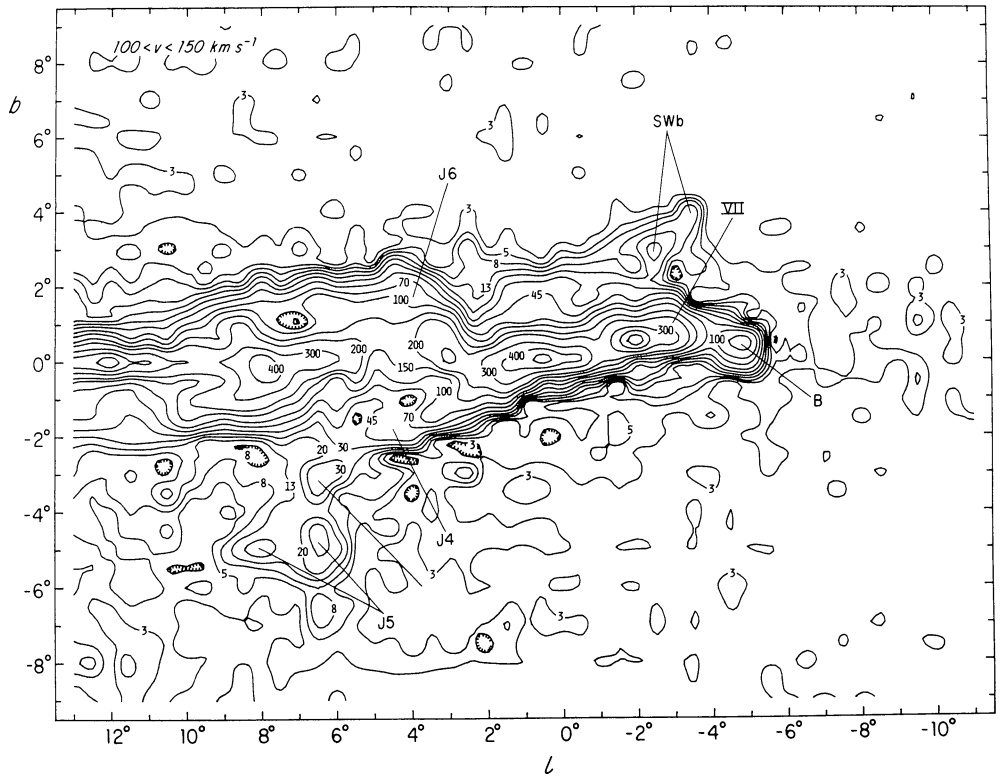

FIGURE 2d. — Map on the plane of the sky of observed HI antenna temperature integrated over the velocity range $100 < v < 150$ km.s^{-1}. The Sanders and Wrixon (1972b) feature is labelled, as are features J4, J5 and J6 of Cohen (1975), van der Kruit's (1970) feature VII, and Bania's (1977) « clump 1 » feature, B. Emission at these velocities is strictly forbidden only at $l < 0°$; especially the emission near $b = 0°$ at $l \gtrsim 5°$ will contain a contribution from conventionally-rotating gas not necessarily associated with the central region.

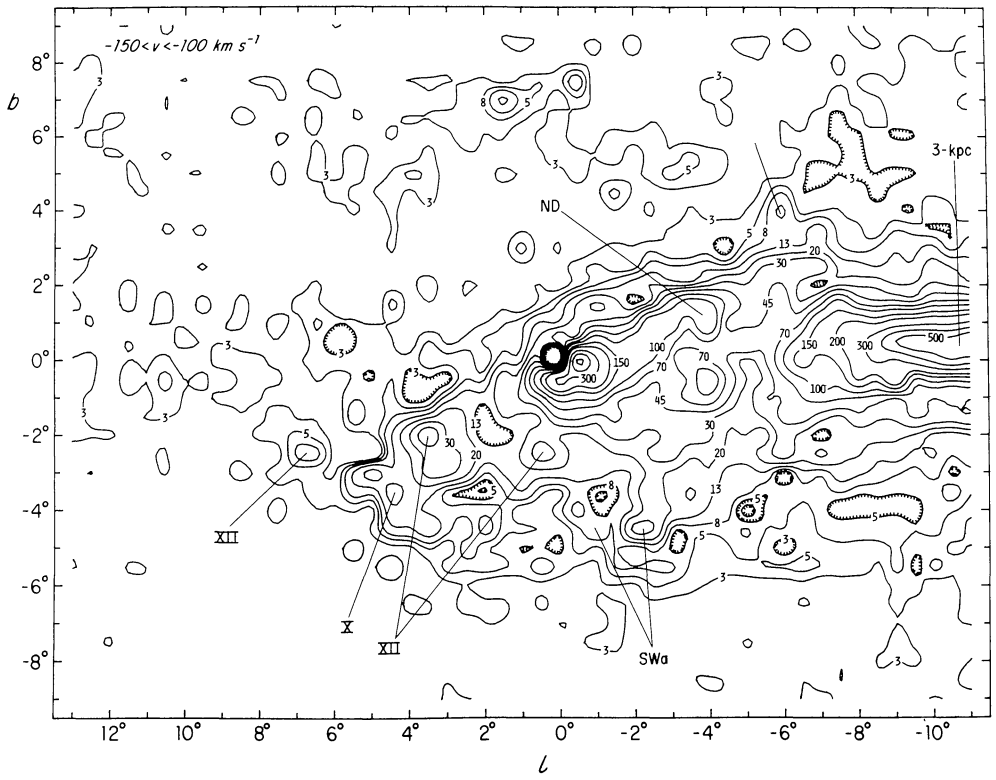

FIGURE 2e. — Map on the plane of the sky of observed HI antenna temperature integrated over the velocity range $-150 < v < -100$ km.s^{-1}. The features labelled include features X and XII of van der Kruit (1970) and the Sanders and Wrixon (1972a) feature, corresponding to J1 of Cohen (1975). Emission contributed by the nuclear disk feature (e.g. Rougoor and Oort, 1960) is indicated. The 3-kpc arm enters this velocity range at $l \lesssim -6°$ near $b = 0°$; that region undoubtedly also contains a contribution from conventionally-rotating gas not necessarily associated with the central region.

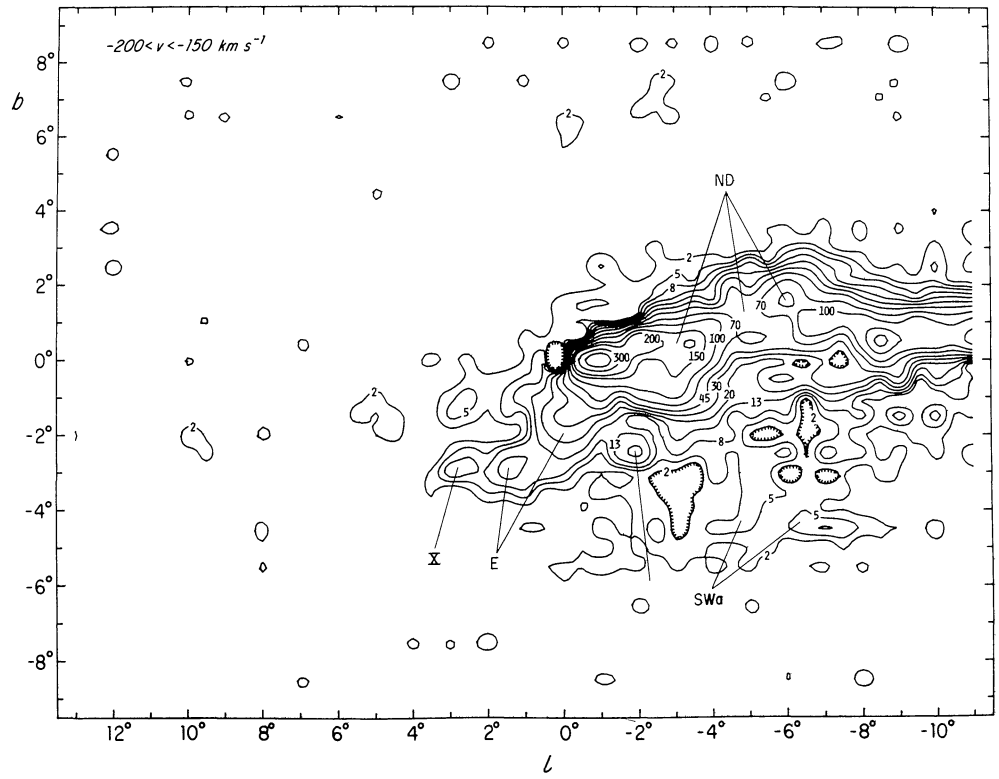

FIGURE 2f. — Map on the plane of the sky of observed HI antenna temperature integrated over the velocity range $-200 < v < -150$ km.s^{-1}. Emission from the nuclear disk is labelled, as are features X of van der Kruit (1970), E of Sanders *et al.* (1972), and SWa of Sanders and Wrixon (1972a).

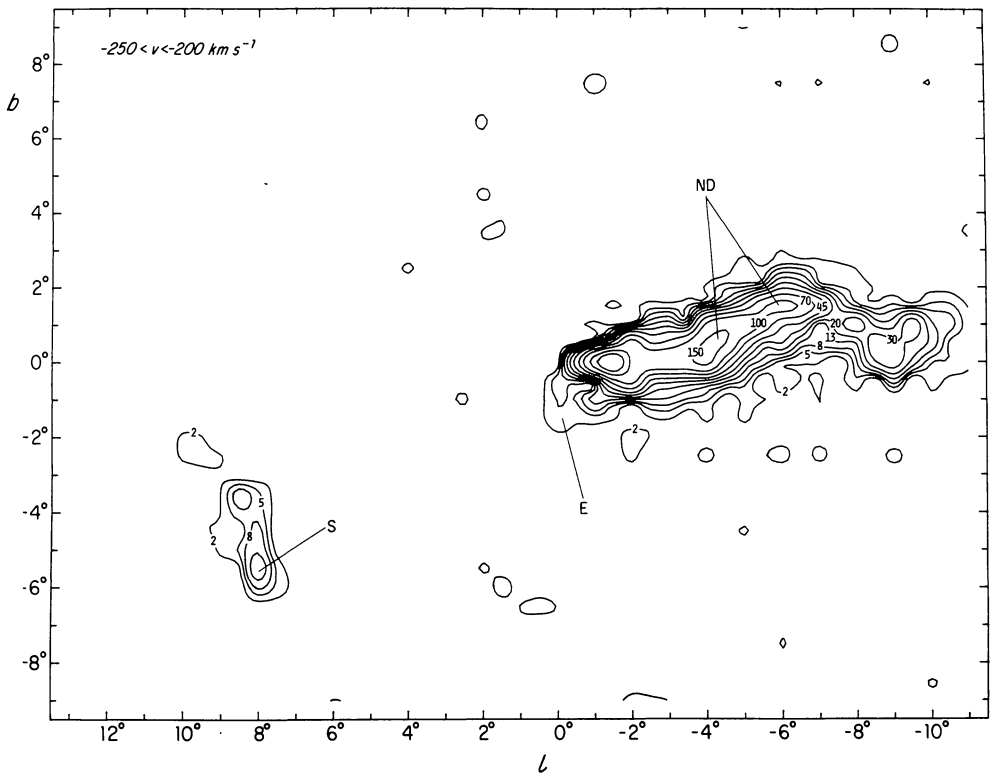

FIGURE 2g. — Map on the plane of the sky of observed HI antenna temperature integrated over the velocity range $-250 < v < -200$ km.s^{-1}. Emission from the nuclear disk, from feature E of Sanders *et al.* (1972), and from Shane's feature (Oort, 1968 ; Hulsbosch, 1968, and Saraber and Shane, 1974) is labelled. The Shane feature differs from the other anomalous features by virtue of its relatively small velocity dispersion and its location outside the kinematic envelope containing the other gas. It shows the characteristics of a high-velocity cloud and thus may have no direct association with the gas in the galactic core.

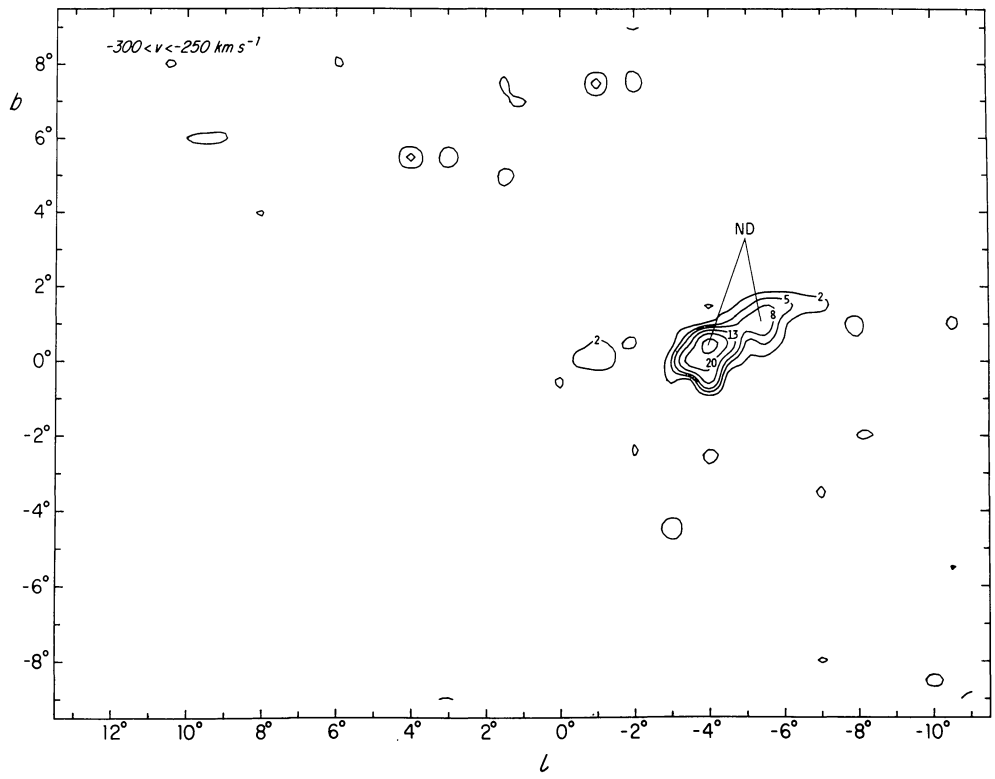

FIGURE 2h. — Map on the plane of the sky of observed HI antenna temperature integrated over the velocity range $-300 < v < -250$ km.s^{-1}. At these extreme velocities only the nuclear disk feature contributes to the spectra.

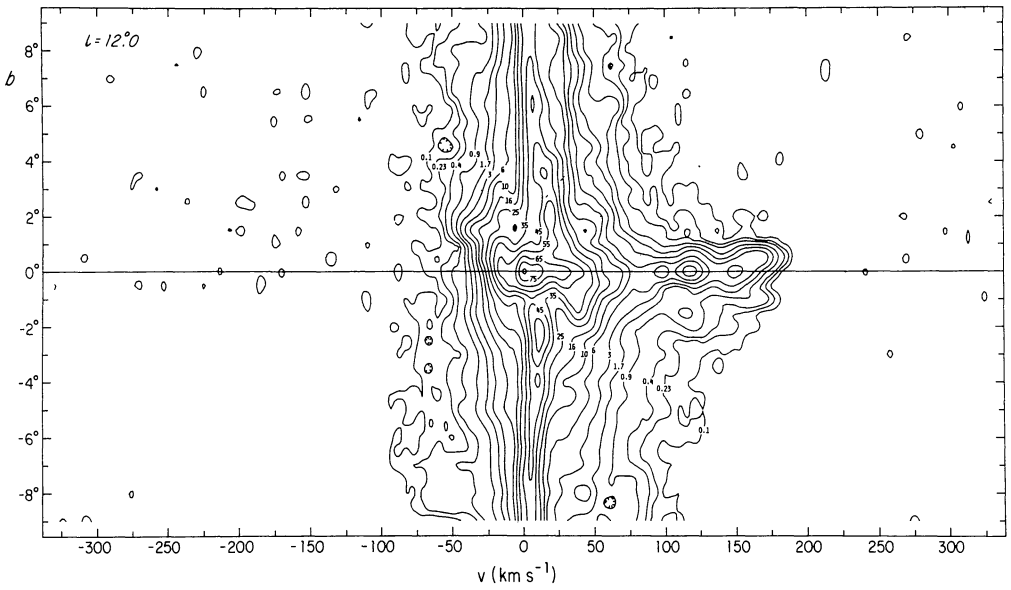

FIGURE 3a. — Contours of antenna temperature in the b, v plane at $l = 12°.0$.

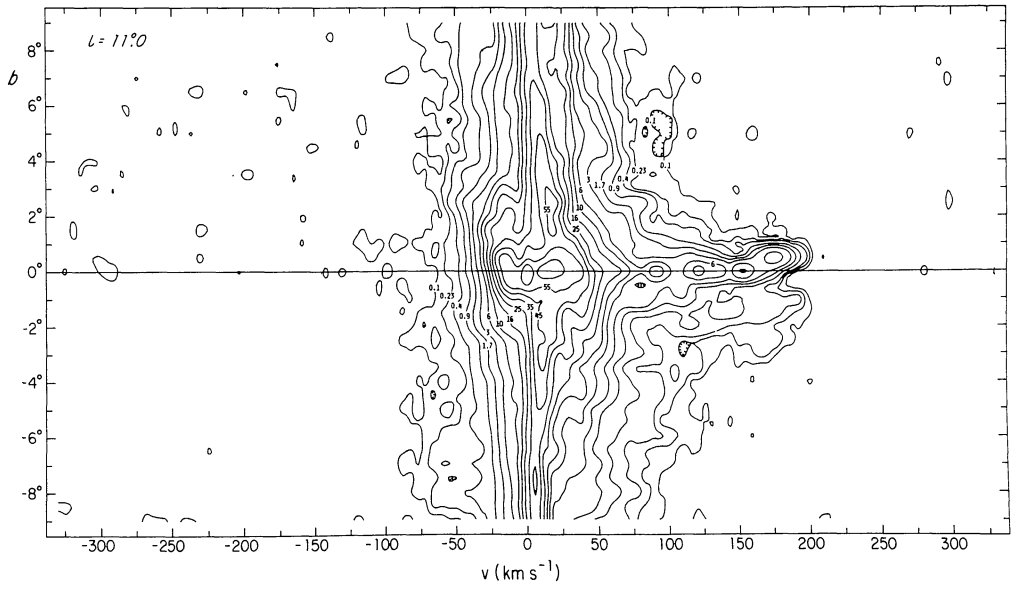

FIGURE 3b. — Contours of antenna temperature in the b, v plane at $l = 11°.0$.

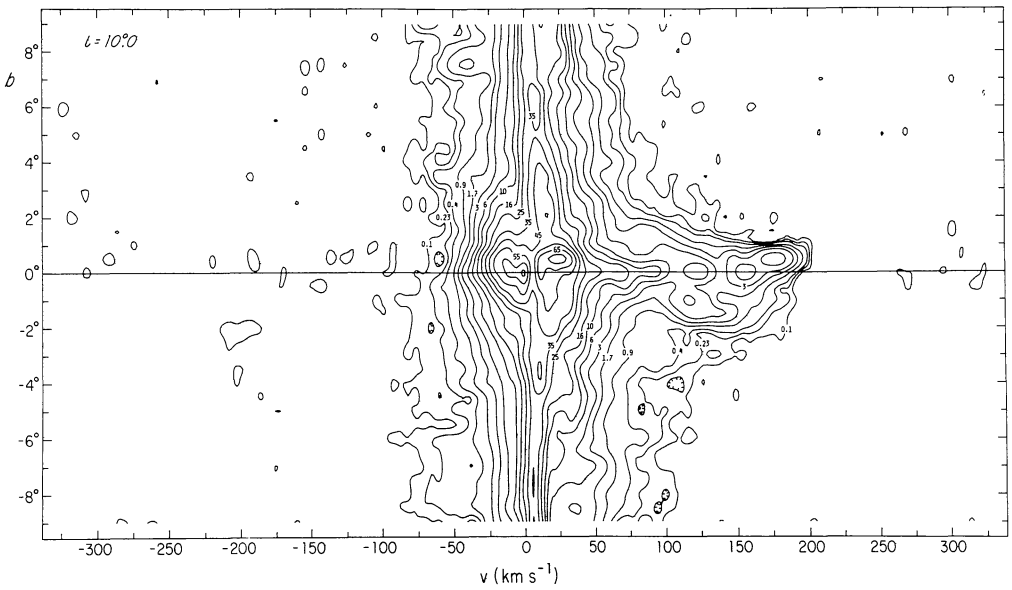

FIGURE 3c. — Contours of antenna temperature in the *b*, *v* plane at $l = 10°0$.

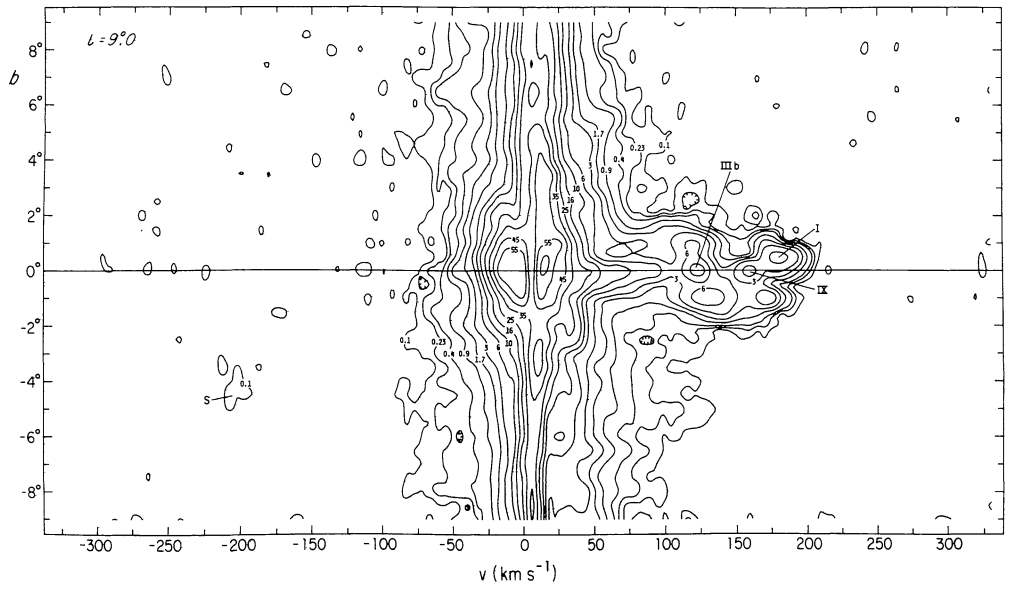

FIGURE 3d. — Contours of antenna temperature in the *b*, *v* plane at $l = 9°0$. The feature labelled S was discovered by Shane (see Oort, 1968 and Hulsbosch, 1968) and is discussed separately by Saraber and Shane (1974). It is discussed by van der Kruit (1970) and by Cohen (1975) as their feature XI. The feature labelled I by Rougoor (1964), van der Kruit (1970), and Cohen (1975) is also often discussed as the « expanding arm at + 135 km.s^{-1} ». Feature IIIb is considered by Cohen (1975) as a branch of the van der Kruit (1970) and Rougoor (1964) feature III. Feature IX is discussed by van der Kruit (1970) and by Cohen (1975).

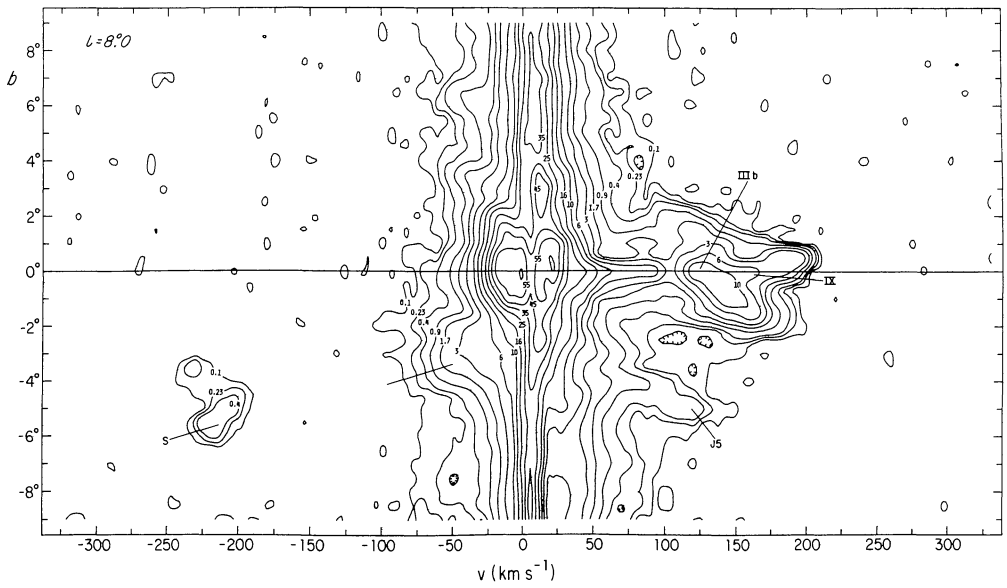

FIGURE 3e. — Contours of antenna temperature in the *b*, *v* plane at $l = 8°.0$. Features S, IIIb, and IX are labelled, as is feature J5, which was first isolated by Cohen (1975).

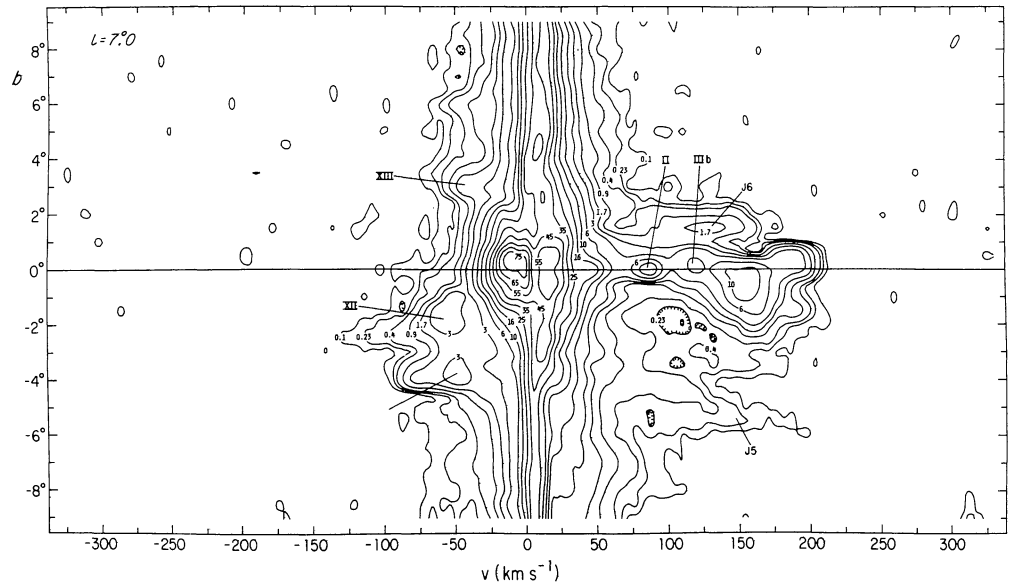

FIGURE 3f. — Contours of antenna temperature in the *b*, *v* plane at $l = 7°.0$. The features labelled XII and XIII were discussed by van der Kruit (1970) ; those labelled J5, J6, and IIIb, by Cohen (1975). Feature II was first discussed by Rougoor (1964), and subsequently by van der Kruit (1979) and Cohen (1975).

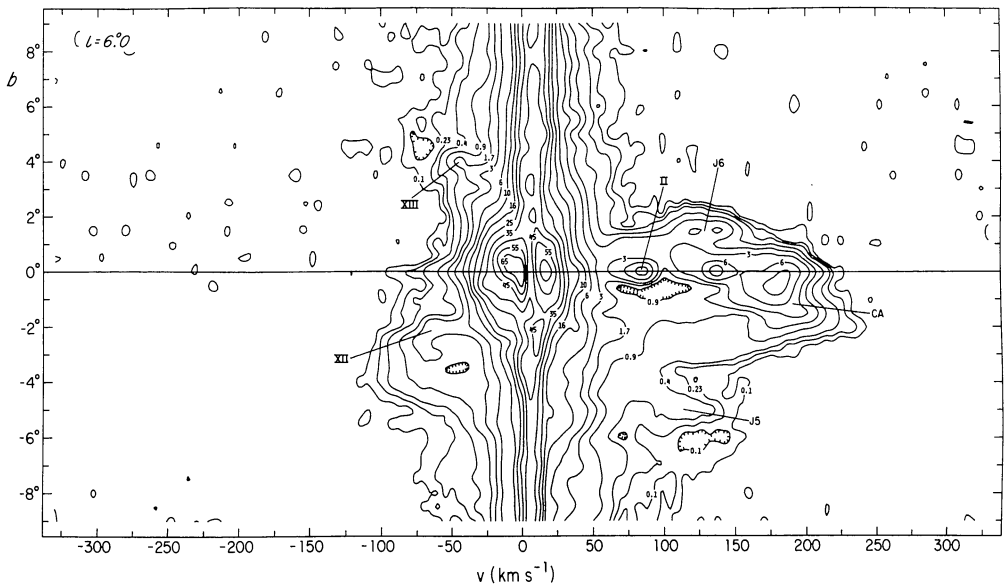

FIGURE 3g. — Contours of antenna temperature in the *b, v* plane at $l = 6°.0$. In addition to the features labelled in figure 3f, the major connecting arm feature discussed by Rougoor (1964) is labelled CA.

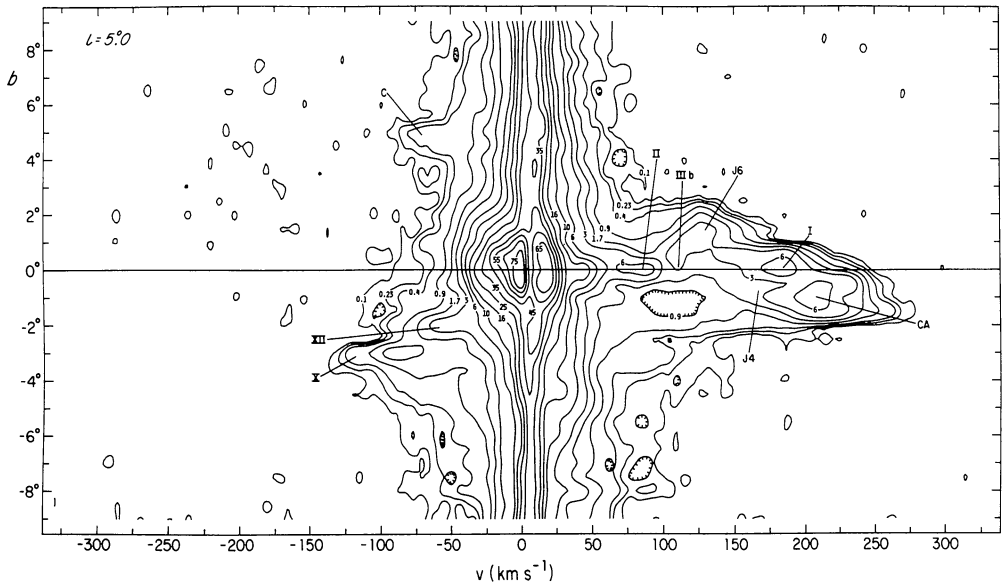

FIGURE 3h. — Contours of antenna temperature in the *b, v* plane at $l = 5°.0$. The van der Kruit (1970) features XII and X, the Cohen (1975) features J4, J6, and IIIb, and the connecting arm feature are labelled. The feature labelled *c* is considered by Cohen to be separate from the nearby features XIII and J3. The Rougoor (1964) features I and II are also labelled.

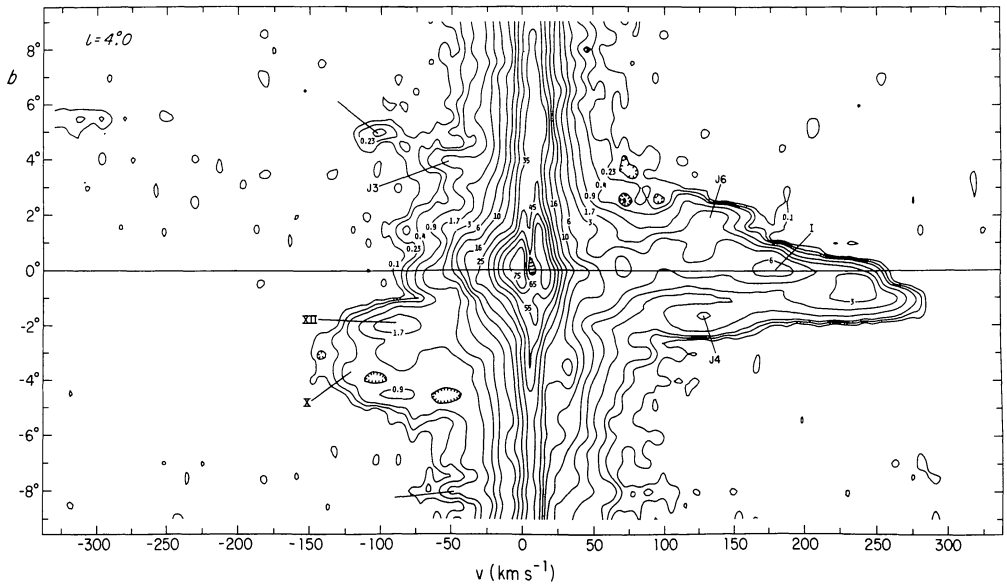

FIGURE 3i. — Contours of antenna temperature in the *b*, *v* plane at $l = 4°.0$. The features labelled include XII and X of van der Kruit (1970) and J3, J4 and J6 of Cohen (1975). J3, which may include emission from van der Kruit XIII, apparently has a low-velocity extension. Feature I is the « expanding arm at + 135 km.s^{-1} » discussed by Rougoor (1964).

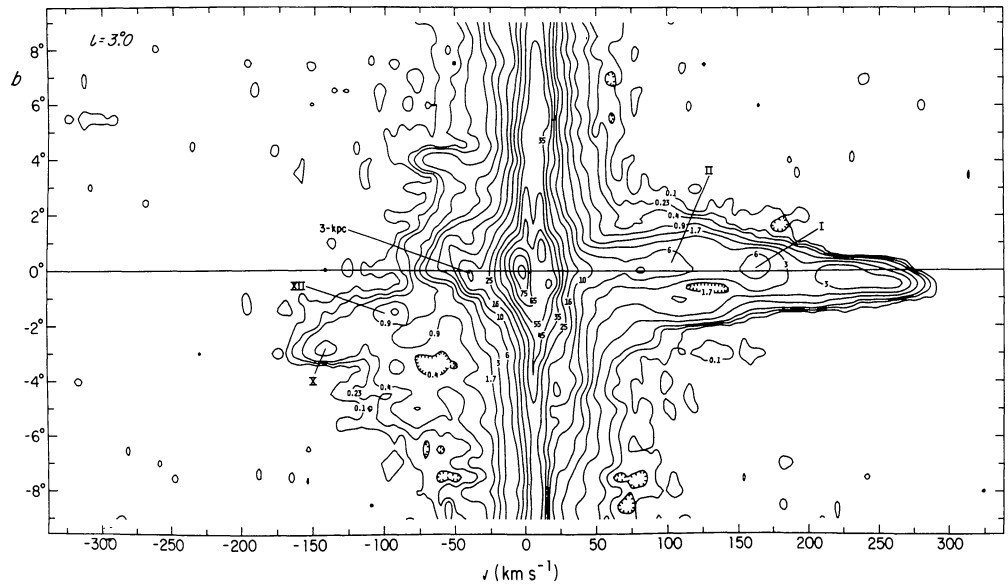

FIGURE 3j. — Contours of antenna temperature in the *b*, *v* plane at $l = 3°.0$. The location of the 3-kpc arm (van Woerden, Rougoor and Oort, 1957 ; Rougoor and Oort, 1960) is indicated in figures 3j - 3x. The feature labelled C is considered by Cohen (1975) to be separate from van der Kruit XIII and from Cohen J3. The van der Kruit (1970) features XII and X are also labelled, as are the Rougoor (1964) features I and II.

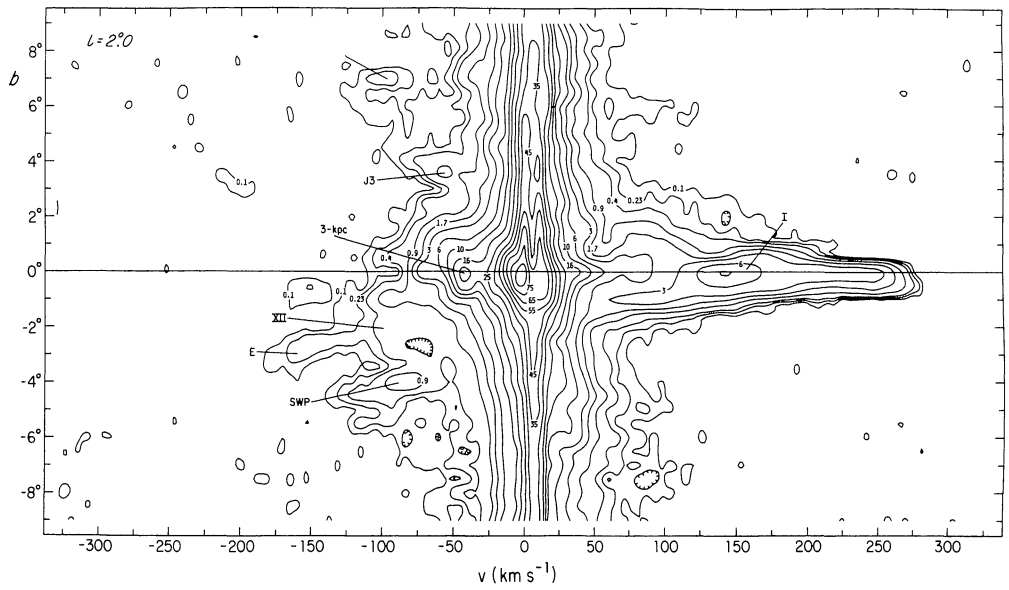

FIGURE 3k. — Contours of antenna temperature in the *b, v* plane at $l = 2°.0$. Sanders, Wrixon and Penzias (1972) first discussed the feature labelled E which they consider to be a weak extension of van der Kruit X. The feature labelled SWP was likewise first discusses by Sanders *et al.* as possibly an extension of van de Kruit XII. The location of Cohen J3 and its extension to more negative velocities and Rougoor's feature I are also indicated.

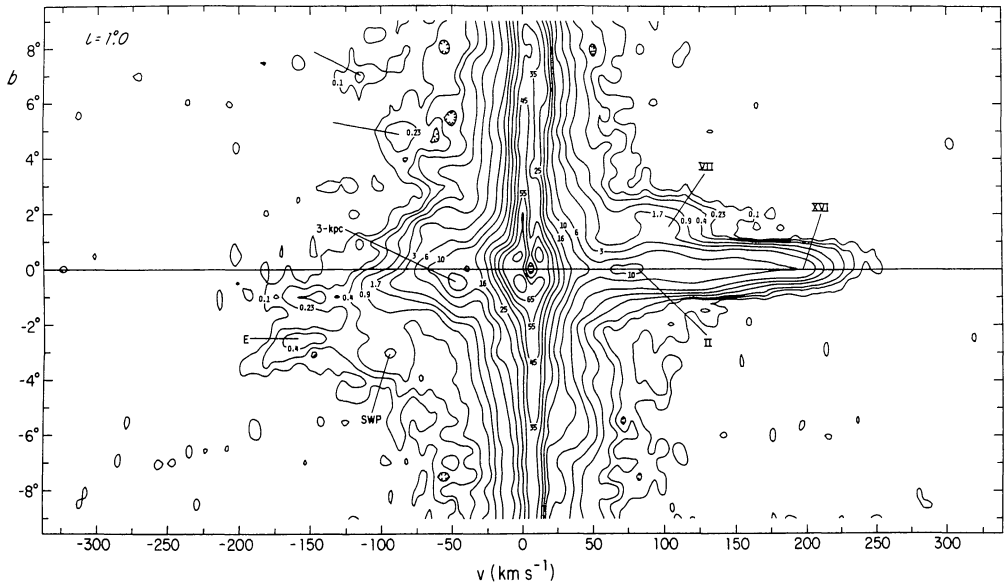

FIGURE 3l. — Contours of antenna temperature in the *b, v* plane at $l = 1°.0$. In addition to the Sanders *et al.* (1972) features E and SWP, the positive-latitude, positive-velocity feature VII of van der Kruit (1970), the Rougoor (1964) feature II, and the feature discussed under the name XVI by van der Kruit (1970) and Cohen (1975) are also indicated. We note here (as is also evident in figures 3k and 3m) that the region $v < 0$ km.s^{-1}, $l \geq 0°$ contains substantial amounts of « forbidden-velocity » gas. This gas has in our opinion been underemphasized in some interpretations of the *l, v* diagram at $b = 0°$ (see figure 4g) because of its displacement to $b < 0°$ and because of the possibly important effects of absorption against continuum sources in the galactic core.

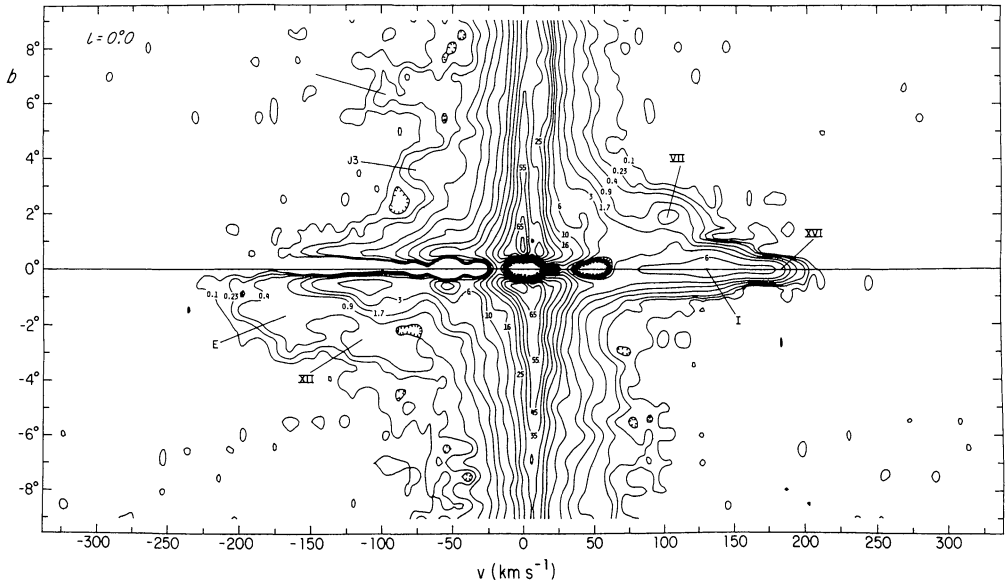

FIGURE 3m. — Contours of antenna temperature in the *b*, *v* plane at $l = 0°.0$. Integration times were lengthened for positions near $|b| < 1°$, $|l| < 4°$, in order to keep the noise level approximately constant in the presence of strong continuum sources. Indicated are Cohen's (1975) feature J3, features E and SWP of Sanders *et al.* (1972), and van der Kruit's (1970) feature VII, Rougoor's (1964) feature I, and van der Kruit's and Cohen's feature XVI. Feature XVI has approximately the same position, velocity behaviour as the « expanding molecular ring » emission (cf. Liszt and Burton 1978).

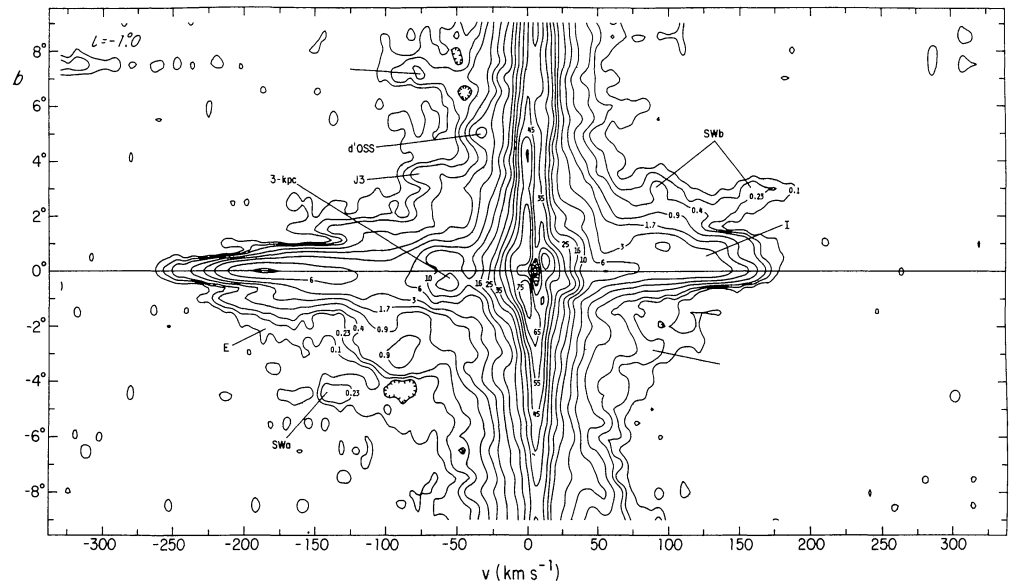

FIGURE 3n. — Contours of antenna temperature in the *b*, *v* plane at $l = -1°.0$. The indicated features are : I (Rougor 1964), SWa (Sanders and Wrixon, 1972a), E (Sanders *et al.*, 1972), J3 (Cohen 1975), d'OSS (d'Odorico *et al.*, 1969), and SWb (Sanders and Wrixon, 1972b). SWa is probably a continuation of XII to negative *l*.

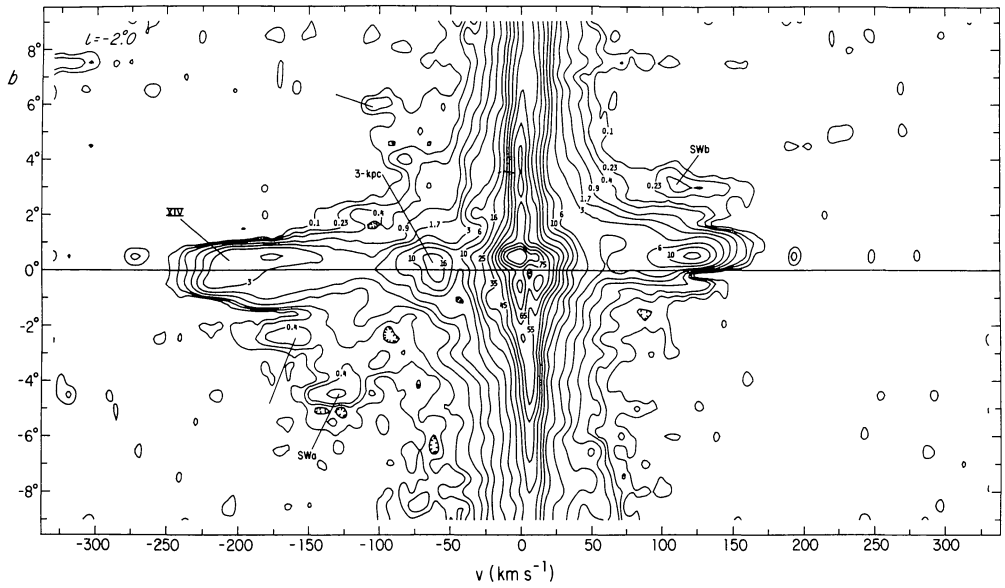

FIGURE 3o. — Contours of antenna temperature in the *b*, *v* plane at $l = -2°0$. The indicated features SWa (Sanders and Wrixon, 1972a) and SWb (Sanders and Wrixon, 1972b) are probably the same features discussed by Cohen (1975) under the headings J1 and J2, respectively. Feature XIV is discussed by van der Kruit (1970) and Cohen (1975).

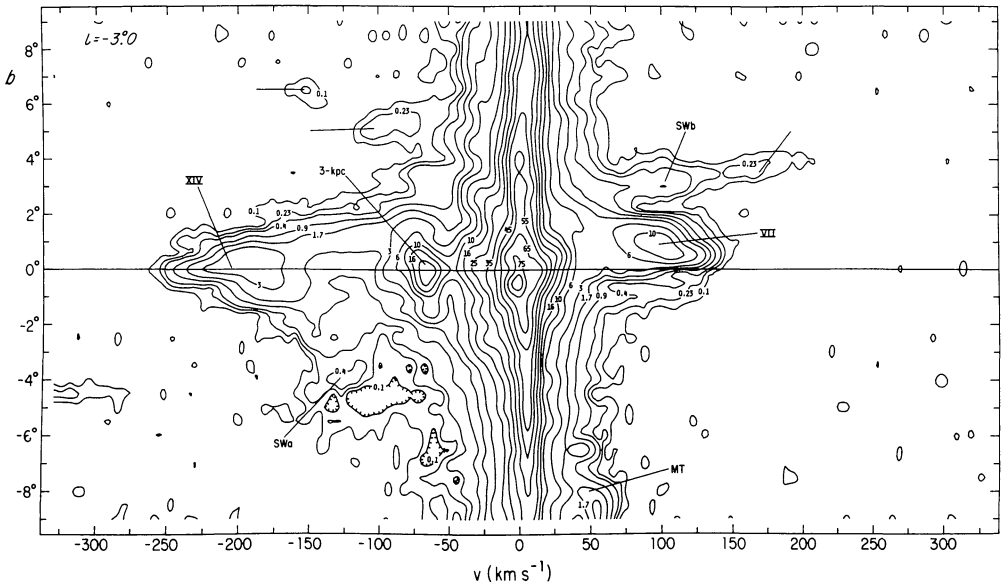

FIGURE 3p. — Contours of antenna temperature in the *b*, *v* plane at $l = -3°0$. In addition to the features referenced in the preceding captions, the low-latitude feature of Mirabel and Turner (1975) is labelled.

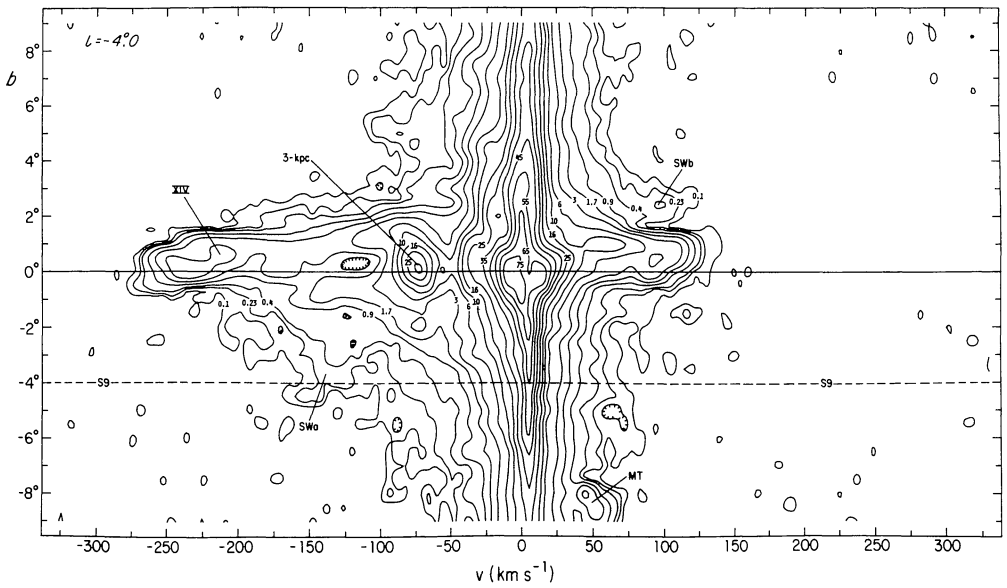

FIGURE 3q. — Contours of antenna temperature in the *b*, *v* plane at $l = -4.^{\circ}0$. The Sanders and Wrixon (1972a, b) and Mirabel and Turner (1975) features are indicated, as in feature XIV of van der Kruit (1970) and Cohen (1975), The label S9 shows the location of the standard-field profile (see Williams, 1973).

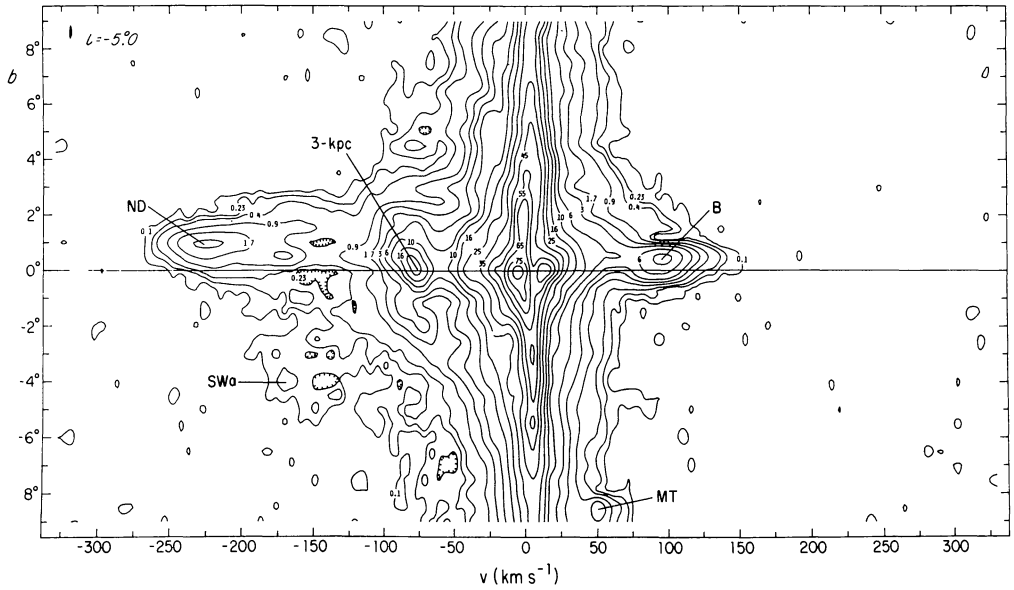

FIGURE 3r. — Contours of antenna temperatures in the *b*, *v* plane at $l = -5.^{\circ}0$. The rather isolated feature labelled B has been discussed by Bania (1977), principally on the basis of CO data. The « nuclear disk » feature first emphasized by Rougoor and Oort (1960) is labelled ND. The features SWa and MT represent continuations of those labelled similarly in the preceding figures.

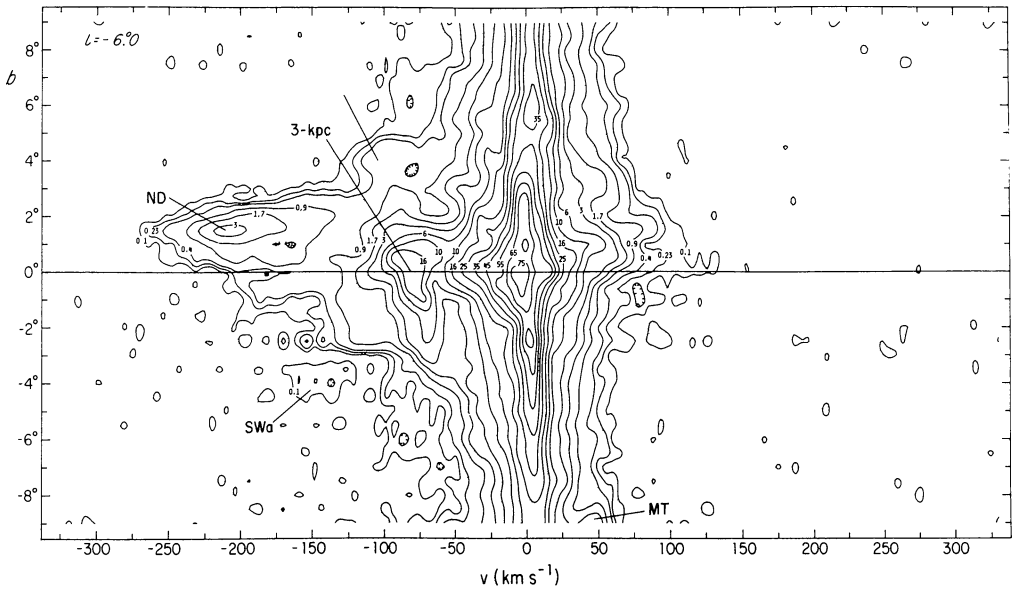

FIGURE 3s. — Contours of antenna temperature in the b, v plane at $l = -6.°0$. The features labelled here are also labelled in the preceding figure.

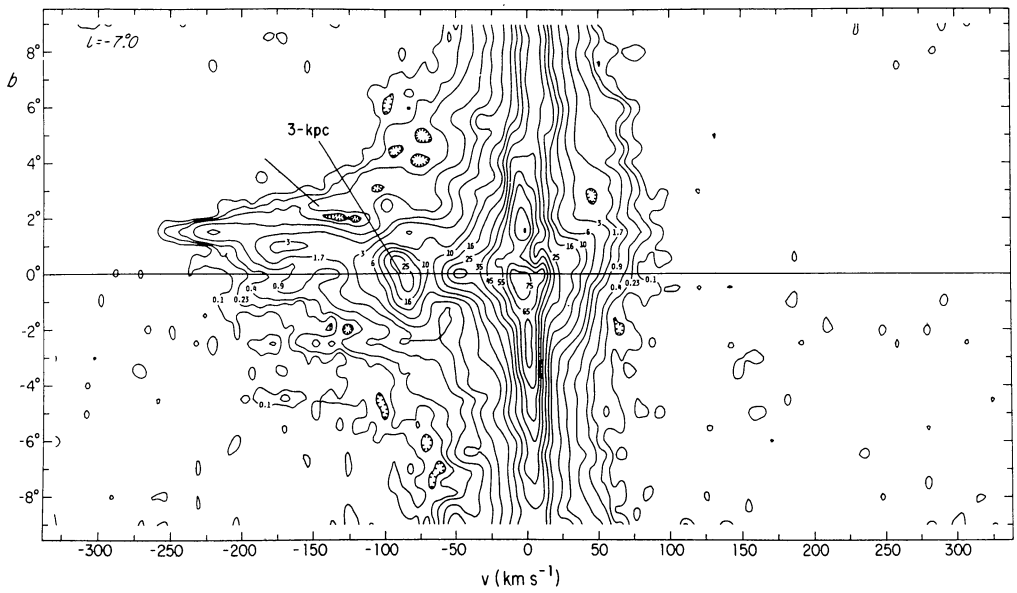

FIGURE 3t. — Contours of antenna temperature in the b, v plane at $l = -7.°0$.

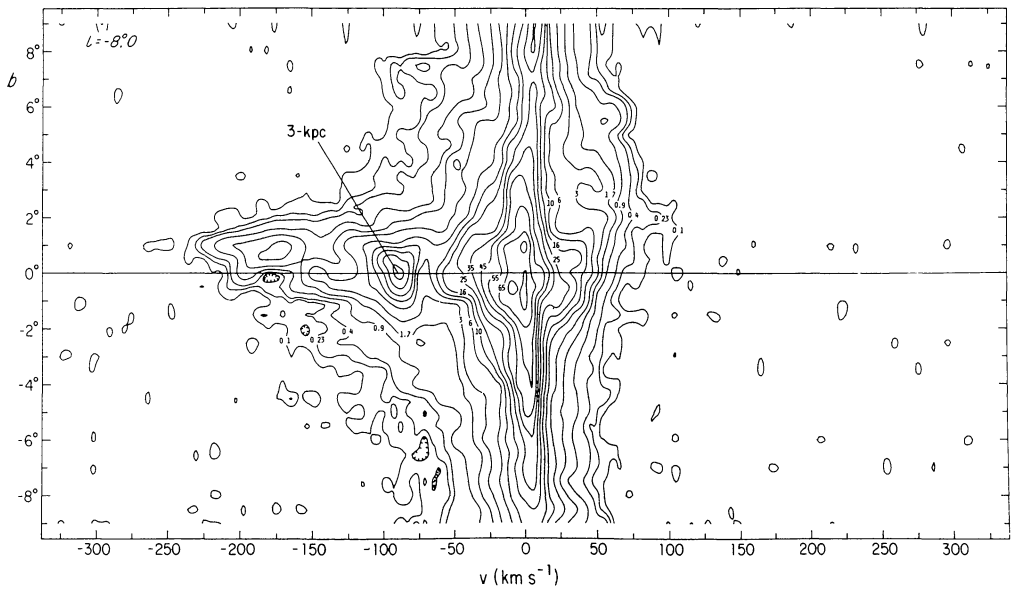

FIGURE 3u. — Contours of antenna temperature in the *b*, *v* plane at $l = -8°0$.

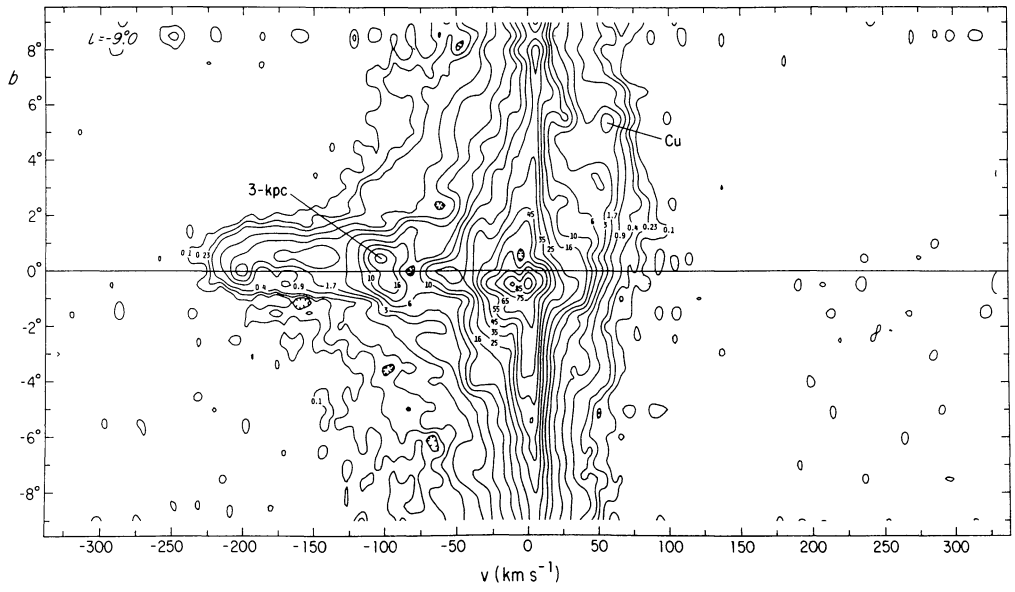

FIGURE 3v. — Contours of antenna temperature in the *b*, *v* plane at $l = -9°0$. Cugnon (1968) first discussed the feature labelled Cu. Subsequent observations of Cugnon's feature have been given by Mirabel *et al.* (1975) and by van der Kruit (1970), who discusses it under the heading feature VIII.

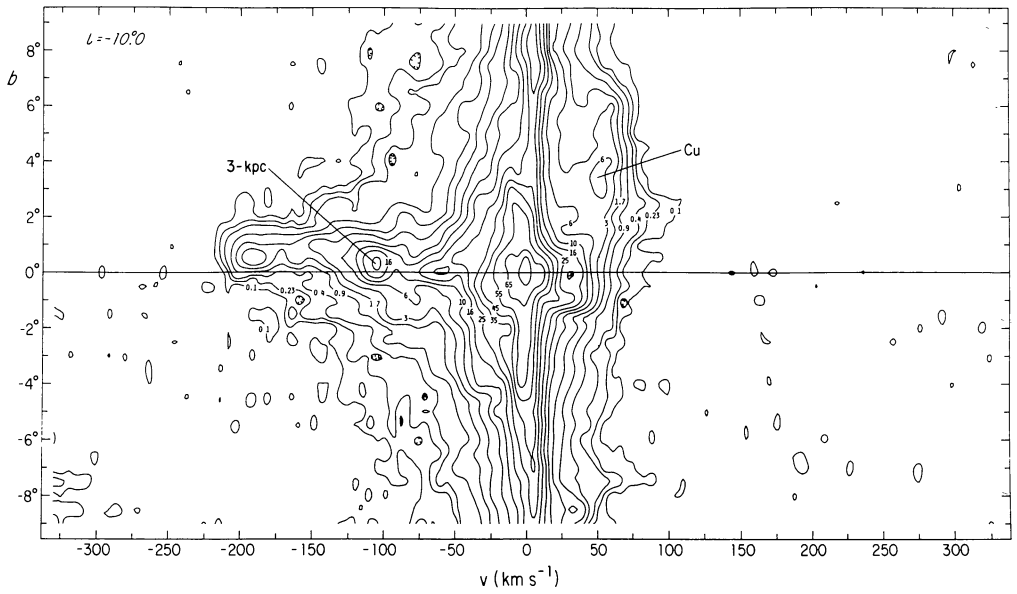

FIGURE 3w. — Contours of antenna temperature in the b, v plane at $l = -10°0$. The location of Cugnon's feature is indicated.

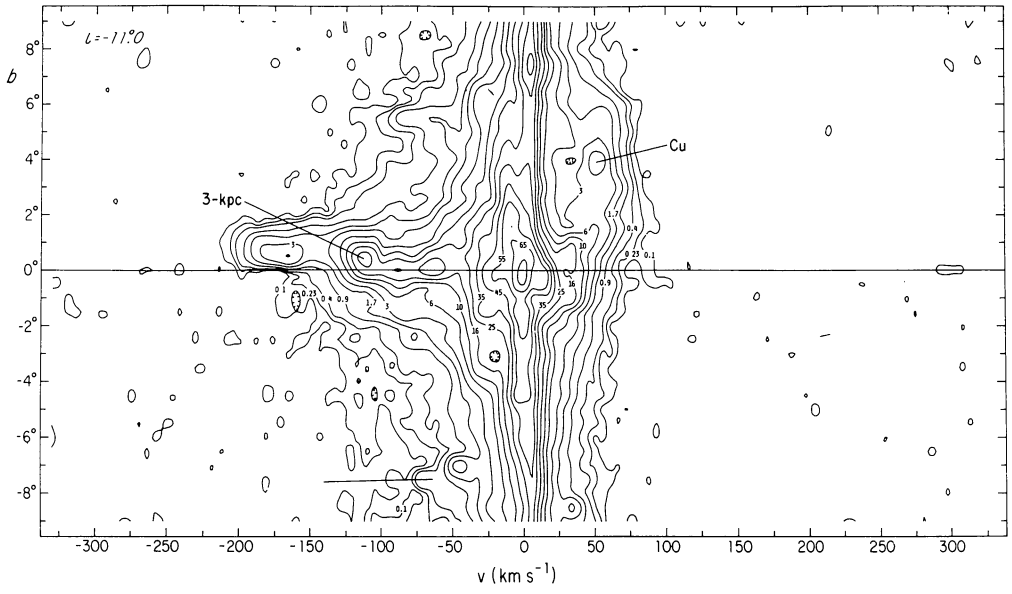

FIGURE 3x. — Contours of antenna temperature in the b, v plane at $l = -11°0$. The location of Cugnon's feature is indicated.

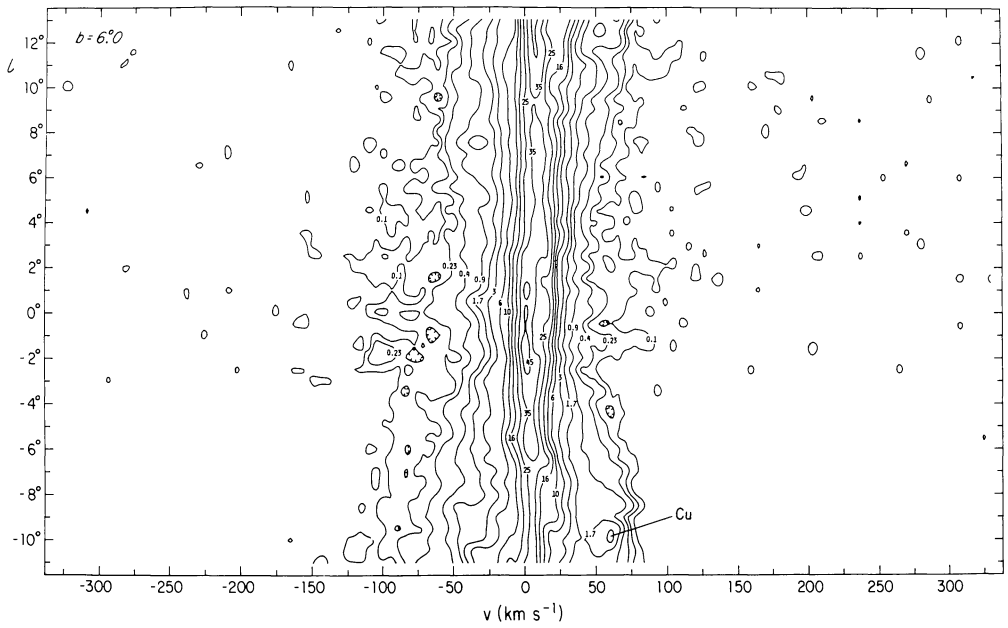

FIGURE 4a. — Contours of antenna temperature in the l, v plane at $b = 6.°0$. The location of Cugnon's feature is indicated.

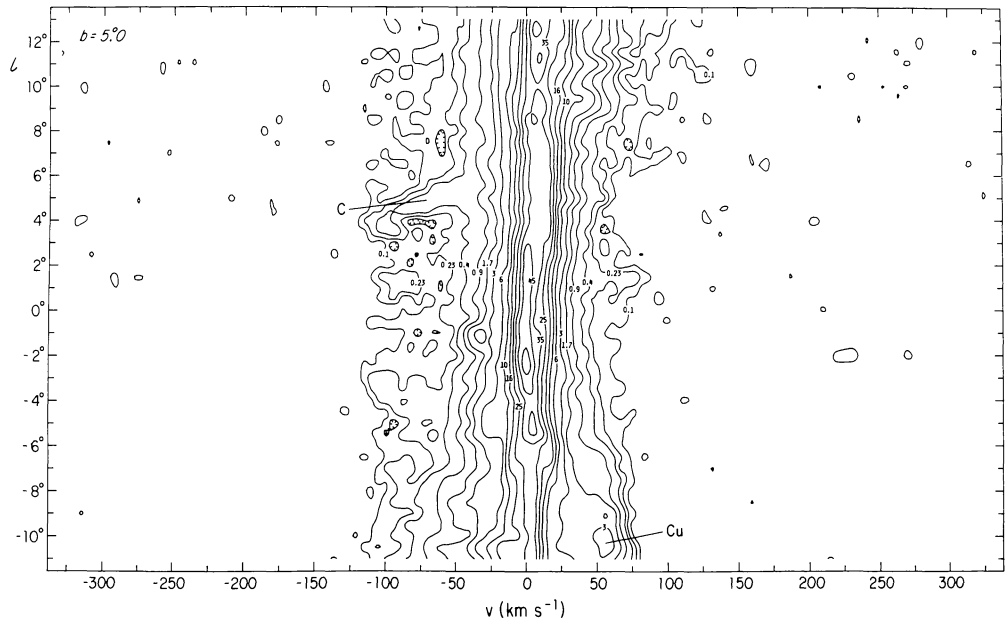

FIGURE 4b. — Contours of antenna temperature in the l, v plane at $b = 5.°0$. The feature labelled C is considered by Cohen (1975) to be separate from the nearby feature XIII (van der Kruit, 1970) and J3 (Cohen, 1975). The location of Cugnon's feature is also indicated.

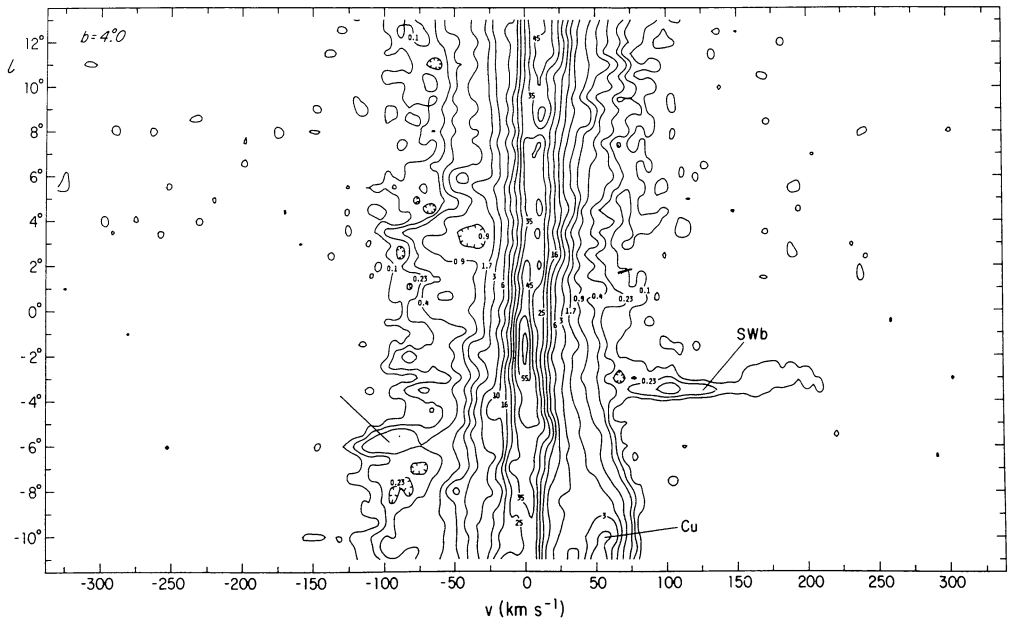

FIGURE 4c. — Contours of antenna temperature in the *l*, *v* plane at $b = 4.^{\circ}0$. Beginning near this latitude and continuing to $b \sim -5.^{\circ}5$ is the regime in which positive-velocity perturbations in the *l*, *v* plane are generally associated with negative-velocity perturbations at the same latitude. In addition to Cugnon's feature, the feature discussed by Sanders and Wrixon (1972b) is labelled ; Cohen's (1975) J2 corresponds to SWb.

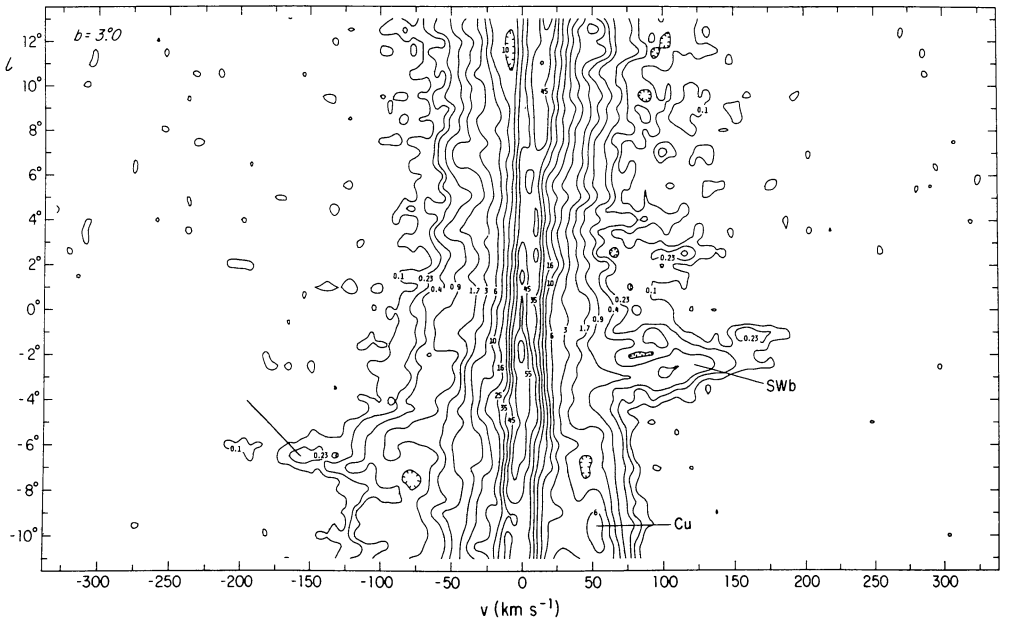

FIGURE 4d. — Contours of antenna temperature in the *l*, *v* plane at $b = 3.^{\circ}0$. The same features are labelled as in Fig. 4c.

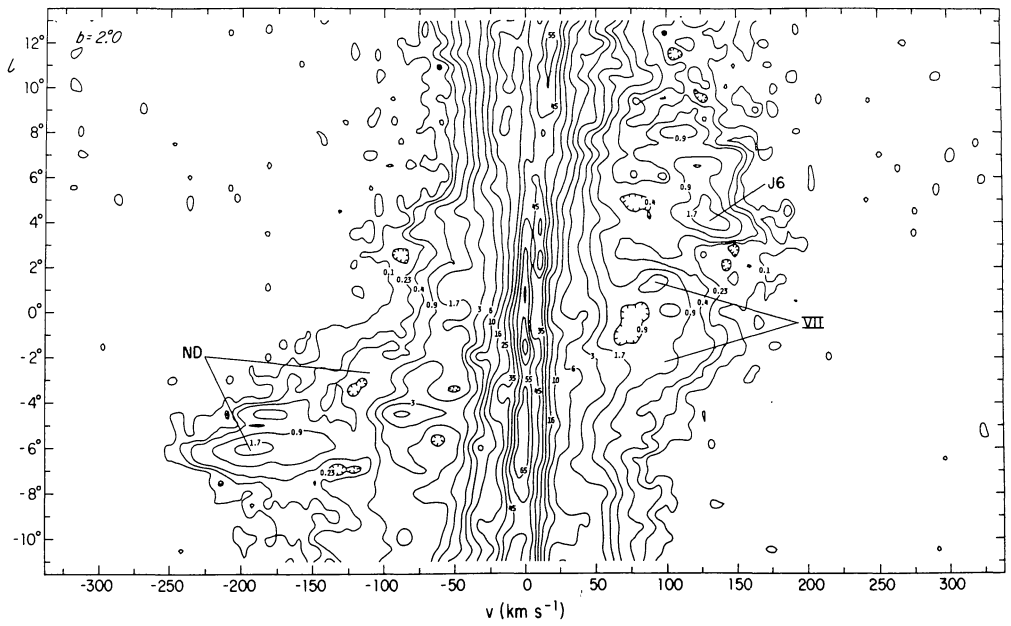

FIGURE 4e. — Contours of antenna temperature in the *l*, *v* plane at $b = 2°0$. Indicated are the Cohen (1975) feature J6, the van der Kruit (1970) feature VII, and emission associated with the nuclear-disk feature.

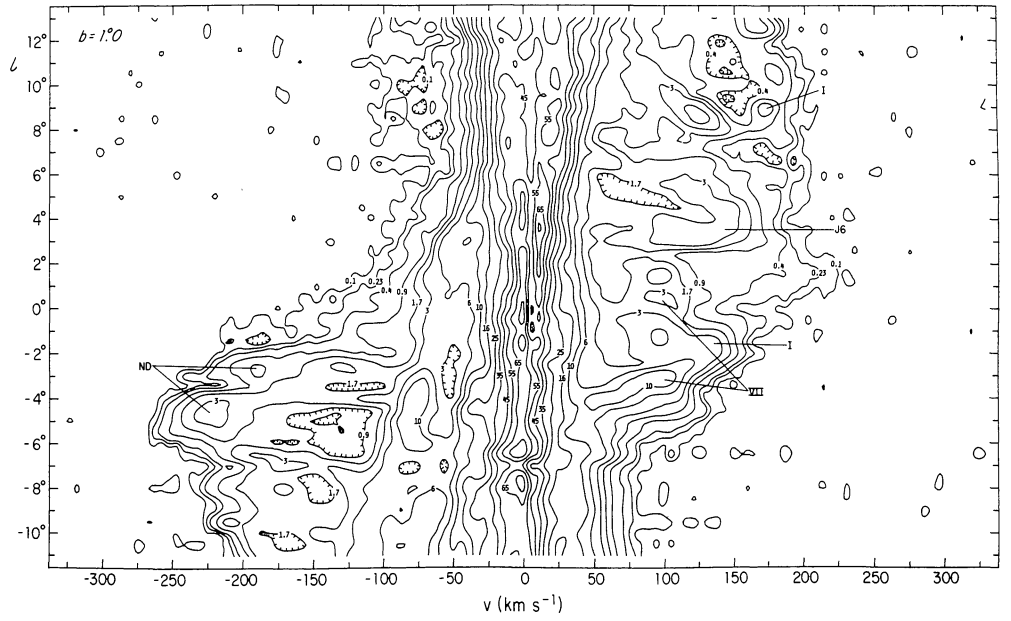

FIGURE 4f. — Contours of antenna temperature in the *l*, *v* plane at $b = 1°0$. In addition to the features labelled in Fig. 4e, feature I of Rougoor (1964), the « expanding arm at + 135 km.s^{-1} », is labelled.

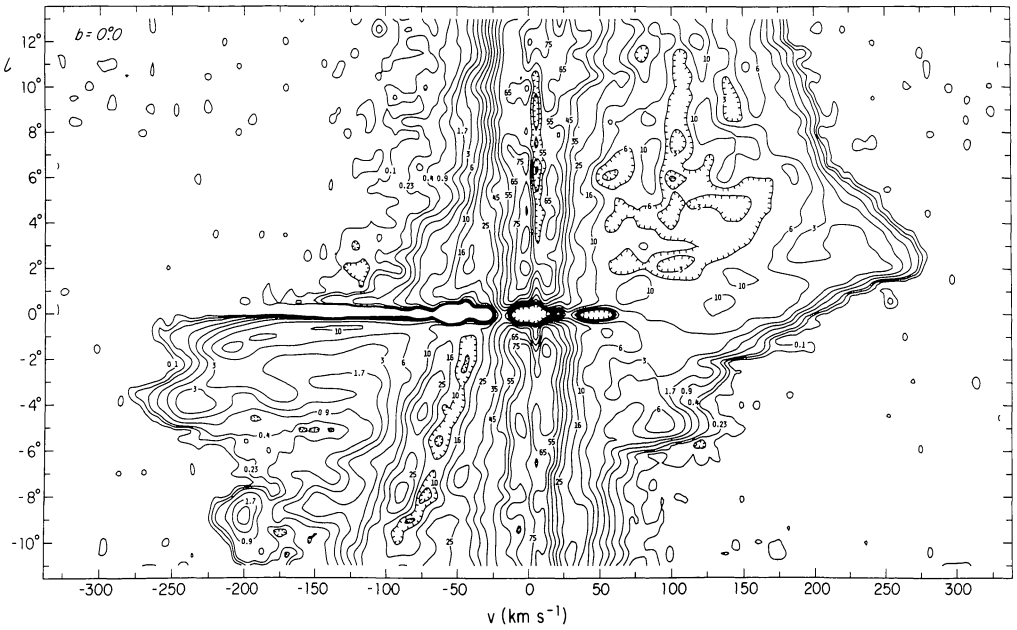

FIGURE 4g. — Contours of antenna temperature in the l, v plane at $b = 0°0$. Integration times were lengthened for positions near $|b| < 1°$, $|l| < 4°$, in order to keep the noise level approximately constant in the presence of strong continuum sources. The influence of absorption against Sgr A is obvious at l, $b = 0°0$. Emission from the region $v < 0$ km.s^{-1}, $l \geq 0°$ has probably been underemphasized in some analyses becauses of its adherence to the core tilt and consequent displacement to $b < 0°$ and because of the possibly important effects of absorption against continuum sources in the galactic core (see Figs. 3k, 3l, 3m ; 4h, 4i).

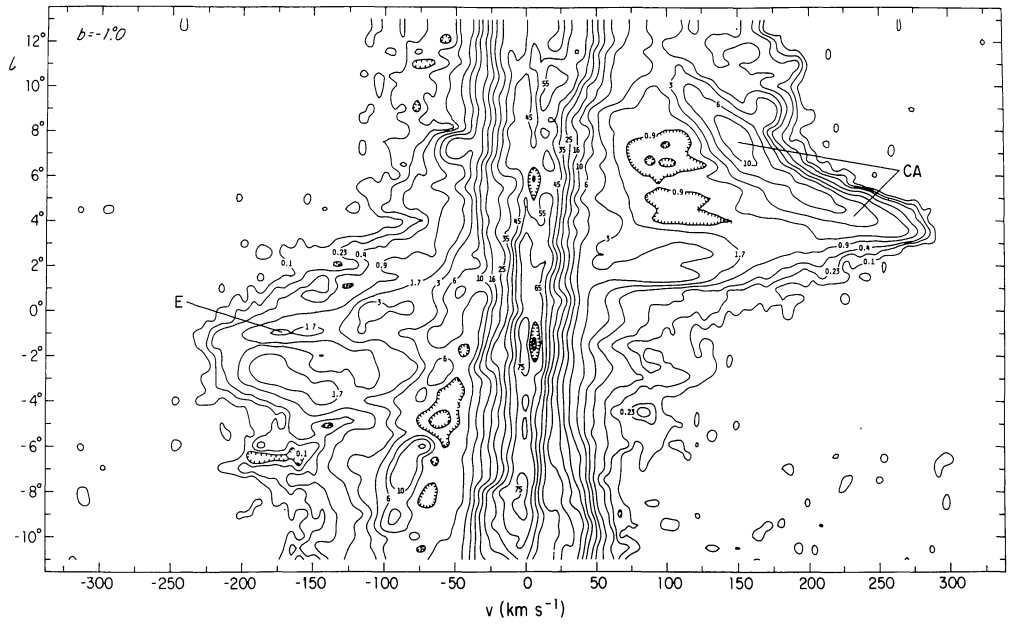

FIGURE 4h. — Contours of antenna temperature in the l, v plane at $b = -1°0$. The Sanders *et al.* (1972) feature E, probably an extension of van der Kruit (1970) X is indicated, as is emission associated with the connecting-arm feature.

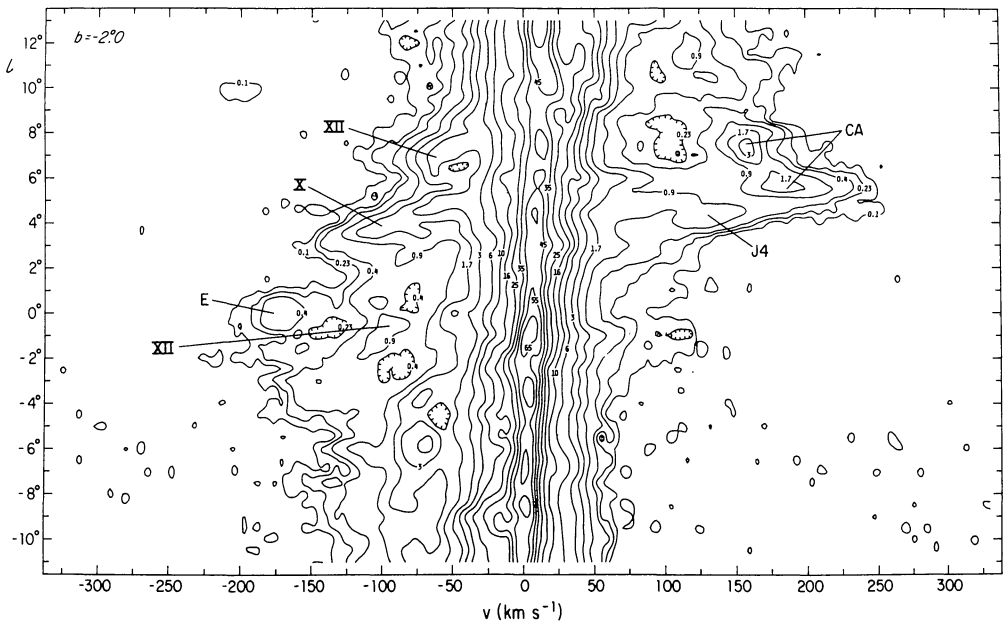

FIGURE 4i. — Contours of antenna temperature in the l, v plane at $b = -2°.0$. Indicated are the van der Kruit (1970) features X and XII, the Sanders *et al.* (1972) feature E, Cohen's (1975) feature J4, and emission associated with the connecting arm.

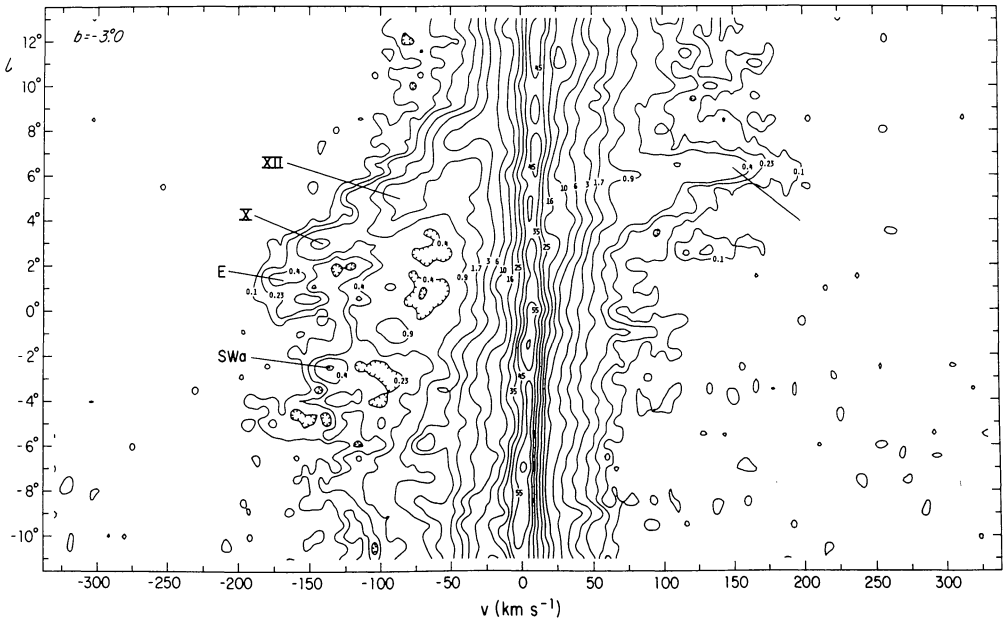

FIGURE 4j. — Contours of antenna temperature in the l, v plane at $b = -3°.0$. The Sanders and Wrixon (1972a) feature is labelled. This feature serves as a good illustration of the suggestion that the emission from the features E, X, and XII is more or less continuous in position, velocity space, and that it may extend to positive velocities.

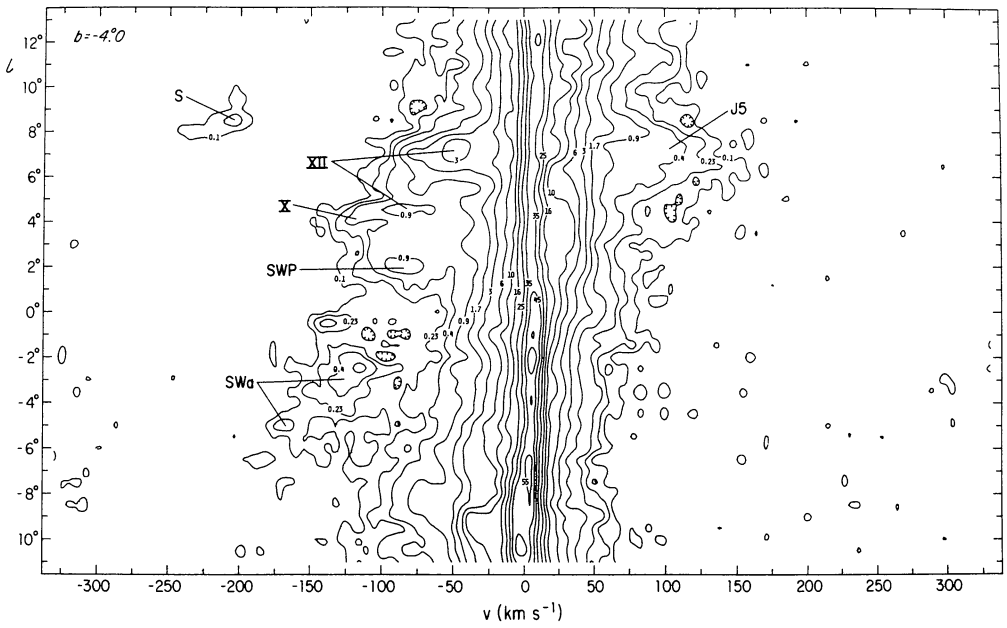

FIGURE 4k. — Contours of antenna temperature in the *l*, *v* plane at $b = -4°0$. The negative-velocity regime shows some continuity of the van der Kruit (1970) features X and XII, the Sanders *et al.* (1972) feature labelled SWP, and the Sanders and Wrixon (1972a) feature SWa. Continuity across zero velocity to the Cohen (1975) feature J5 is suggested. The anomalous feature S was discovered by Shane (see Oort, 1968, Hulsboch, 1968, and Saraber and Shane, 1974).

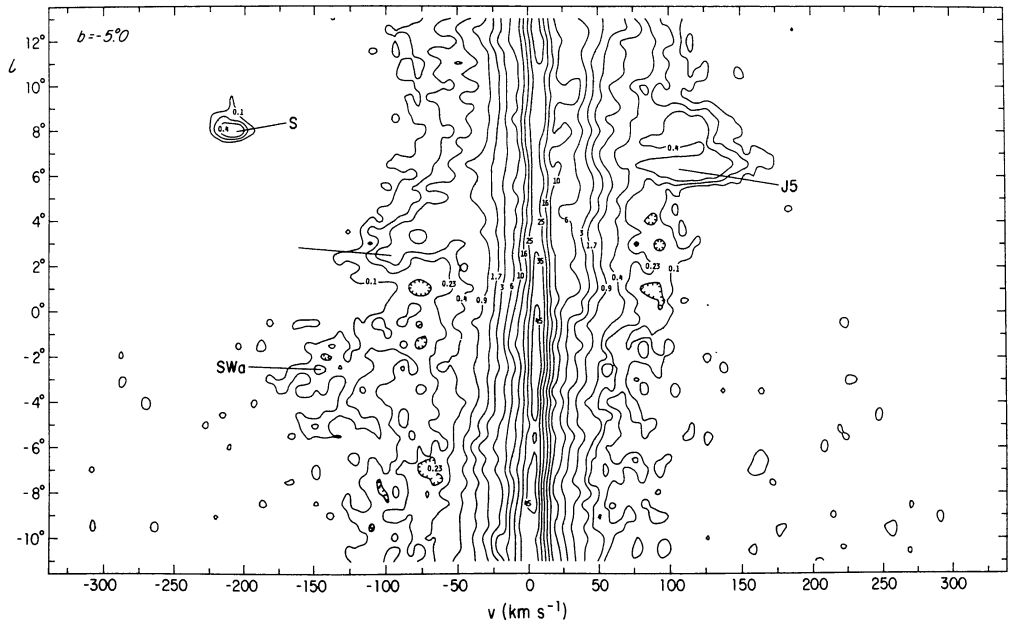

FIGURE 4l. — Contours of antenna temperature in the *l*, *v* plane at $b = -5°0$. Cohen's (1975) feature J5 is labelled and the location of its possible negative-velocity counterpart is indicated. Also labelled are Shane's feature S and the Sanders and Wrixon (1972a) feature SWa.

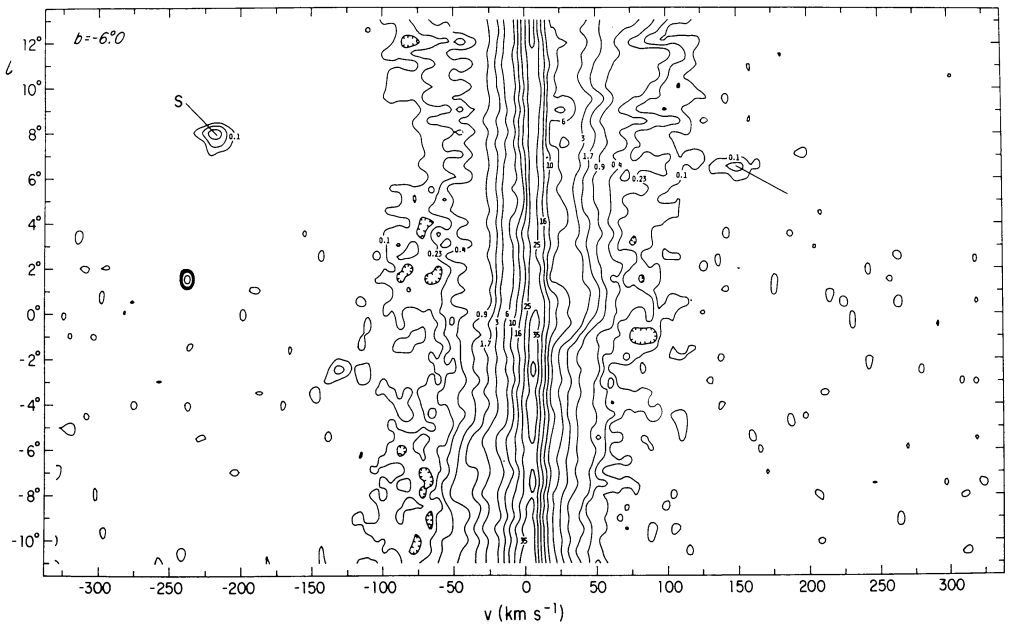

FIGURE 4m. — Contours of antenna temperature in the l, v plane at $b = -6°0$. The location of Shane's feature is labelled. (The intense peak near $l = 1°5$, $v = -235$ km.s^{-1} is probably due to interference).